Desalination and Water Treatment
www.deswater.com
doi: 10.1080/19443994.2016.1149111

57 (2016) 25114–25139
November

Taylor & Francis
Taylor & Francis Group

Biosorption of Pb(II), Ni(II) and Cr(VI) ions from aqueous solution using *Rhizoclonium tortuosum*: extended application to nickel plating industrial wastewater

S. Suganya[a], K. Kayalvizhi[b,*], P. Senthil Kumar[a,*], A. Saravanan[a], V. Vinoth Kumar[c]

[a]*Department of Chemical Engineering, SSN College of Engineering, Chennai 603110, India, Tel. +91 9159690215; email: sugish18@gmail.com (S. Suganya), Tel. +91 9884823425; email: senthilchem8582@gmail.com (P. Senthil Kumar), Tel. +91 9003838356; email: sara.biotech7@gmail.com (A. Saravanan)*
[b]*District Environmental Engineering Department, Tamilnadu Pollution Control Board, Ambattur, Chennai 600058, India, Tel. +91 8870470685; email: kayalk80@gmail.com*
[c]*Bioprocess Laboratory, Department of Biotechnology, School of Bioengineering, SRM University, Kattankulathur, Chennai 603203, India, Tel. +91 9943764794; email: vinothkumar.v@ktr.srmuniv.ac.in*

Received 24 November 2015; Accepted 28 January 2016

ABSTRACT

The adsorption of Pb(II), Ni(II), and Cr(VI) ions onto *Rhizoclonium tortuosum* (RT) was investigated in a batch mode operation. The two parameter (Langmuir and Freundlich) and three parameter models (Redlich–Peterson and Sips isotherm model) were used to depict the adsorption of metal ions onto *R. tortuosum*. Sips isotherm model was provided the best fit to the adsorption equilibrium data. The adsorption kinetics was described by the pseudo-first-order, pseudo-second-order, and Elovich kinetic models. The pseudo-second-order model provides the best fit. The maximum monolayer adsorption capacity of the RT were found to be 66.08, 85.09, and 61.45 mg/g for Pb(II), Ni(II), and Cr(VI), respectively. The thermodynamic results showed that the adsorption process was endothermic, feasible, and spontaneous in nature. The ability of RT to remove the Ni(II) ions in column studies was explored. The effect of bed height, flow rate, and initial Ni(II) ion concentration were studied. The dynamic behavior of the column performance was studied using the bed depth service time (BDST) and Thomas models. This research was also further extended to treat the nickel contaminated plating industrial wastewater. The results showed that the RT can be utilized as better biosorbent for the removal of metal ions from industrial wastewater.

Keywords: Adsorption; Fixed bed column; Isotherms; Kinetics; *Rhizoclonium tortuosum*; Thomas model

1. Introduction

Heavy metal pollution has become the most important environmental problem today. The main reason for the water pollution is because of the rapid growth of industries, environmental changes, and anthropogenic activities. Rapid development of several industries such as tannery, fertilizer, metal plating, leather, fuel production, paints, coal, paper, galvanizing, non-ferrous alloys,

*Corresponding authors.

mining, metallurgical, photography, dyes, electroplating, battery, and pigment industries are the major sources for the heavy metal pollution [1,2]. These industries discharge the numerous metal ions directly into the water streams. Heavy metals such as lead, nickel, chromium, zinc, copper, and cadmium are stable, carcinogenic, bioaccumulation, non biodegradable, and may accumulate in micro-organism. Among these, Pb (II) and Ni(II) and Cr(VI) ions are deemed to be highly toxic [3,4]. The source, effects of these heavy metals and their maximum contamination level is shown in Table 1. These heavy metals are reported as priority pollutants which can be easily enter into the human food chain due to their toxicity and mobility. These heavy metals causes serious health problems which includes lung irritation, skin irritations, diarrhea, kidney damage, dermatitis, bone cancer, headache, liver damage, nervous system problem, and vomiting to humans [5]. Normally industrial wastewater contains Pb(II), Ni(II), and Cr(VI) metal ions in the range of 5–15 mg/L, 2–200 mg/L, and 0.5–270 mg/L, respectively. The legal limits of Pb(II), Ni(II), and Cr(VI) ions concentration for drinking water and surface water is 0.05 and 0.1 mg/L, 0.01 and 2 mg/L, 0.05 and 0.2 mg/L, respectively [6]. Consequently, controlling the discharge amount of Pb(II), Ni (II), and Cr(VI) ions from the industrial effluent is much more important for human health. Several conventional methods have been employed for the removal of heavy metals from aqueous solution which includes chemical precipitation, electrodialysis, membrane separation, chelation, reverse osmosis, ion exchange, and ultrafiltration [7–9].

These methodologies have several drawbacks such as cost expensive, sludge disposal problems, low efficiency, and time-consuming process [10–12]. Biosorption is the promising technology for the effective removal of heavy metals from aqueous solution. This biosorption process has several advantages compared to other metal remediation process such as high efficiency performance at low concentration, low-cost operation, no sludge formation, and easy handling process [13]. Many researchers have been stated that the freshwater and marine algae as good adsorbent material for the sequestration of heavy metals from aqueous solution. Algae are the low-cost naturally available adsorbent material and have remarkable metal uptake capacity. Algae plays a significant role in the adsorption process, the cell wall of the algae is composed of polysaccharides, proteins, and lipids. Several functional groups such as amino, hydroxyl, carboxyl, and sulfate present on the cell wall of the algae that assist the heavy metal adsorption by electrostatic attraction [14–17].

In this present study, *Rhizoclonium tortuosum* (RT) species have been used as biosorbent for the removal of Pb(II), Ni(II), and Cr(VI) ions from aqueous solutions. The objective of the present research work is to develop a low-cost adsorbent (*R. tortuosum*) for the effective removal of metal ions from aqueous solutions. Biosorption of Pb(II), Ni(II), and Cr(VI) ions in batch adsorption experiment were carried out and the process parameters such as solution pH and temperature were optimized. The experimental data were applied to the two-parameter (Langmuir and Freundlich) and three-parameter (Redlich–Peterson and Sips) adsorption isotherm models to check the biosorption process. The adsorption kinetic studies were carried out using pseudo-first-order, pseudo-second-order, and Elovich kinetic models. The thermody-

Table 1
Source, effects, and maximum contamination level of Pb(II), Ni(II), and Cr(VI) ion contaminations

S. no.	Industry	Heavy metal	Toxicity	MCL (mg/L)
1	Paints and pigments, batteries, electronics, fertilizers, alloy and steels, sewage sludge, paper and pulp, and landfill leachate	Lead (Pb)	Damages in nervous system, circulatory system, kidney damage, Alzheimer's disease, and decreased bone growth	0.006
2	Alloy and steels, batteries, electroplating, electronics, mining, sewage sludge, paper and pulp, and landfill leachate	Nickel (Ni)	Dermatitis, asthma, cancer risk, respiratory disorders, neuronal disorder, and metal fume fever	0.20
3	Electroplating, paints and pigments, electronics, mining, fertilizers, sewage sludge, landfill leachate, leather, photography, and tannery	Chromium (Cr)	Lung cancer, bone cancer, diarrhea, damage of kidney, liver, nervous system, skin irritation, dermatitis, mutagenicity, and carcinogenicity	0.05

Note: MCL—maximum contamination level.

namic studies were also investigated for the adsorption process. The column design parameters such as bed height, flow rate, and initial metal ions concentration were optimized which explored the adsorption of Ni(II) ions in the fixed bed column.

2. Materials and methods

2.1. Collection and preparation of biosorbent

Selected algae species—*R. tortuosum* (RT) were collected from pond, wells, and pools of water near Dharmapuri, Tamilnadu, India. The algae biomass (RT) was expansively washed with distilled water to remove the impurities such as sand and other debris. The washing was continued two to three times to remove the impurities entirely from the algae species. Then the washed algae biomass (RT) was completely dried under the sunlight for 10 d. After drying, the biomass material was grounded into fine powder. This ensuring material was further treated with 0.1 N HCl for about 5 h in orbital shaker at 150 rpm. Then the dehydrated algae biomass (RT) was washed with distilled water to remove the excess acid content in the algae biomass. Finally, the obtained adsorbent material (RT) was dried in the hot air oven at 60°C for about 24 h. The resulting adsorbent material (RT) was used as a biosorbent with an average particle size of 0.7 mm for the effective removal of Pb(II), Ni(II), and Cr(VI) ions from the aqueous solutions.

2.2. Characterization techniques

The surface morphology of the algae species (RT) were characterized by Fourier transform infrared spectroscopy (FTIR) and scanning electron microscopy (SEM). The interaction between the chemical bonds and the metal ions on the surface of the adsorbent material (RT) was examined using FTIR within the range of 450–4,000 cm^{-1}. The surface structure and morphology of the adsorbent material were characterized by SEM analyses under an accelerating voltage of 10 kV.

2.3. Adsorbate

Lead nitrate ($Pb(NO_3)_2$), nickel sulfate hexahydrate ($NiSO_4{\cdot}7H_2O$), and potassium dichromate ($K_2Cr_2O_7$) were supplied from E. Merck, India. The stock solution of Pb(II), Ni(II), and Cr(VI) ions were prepared by dissolving the measured quantities of salts such as Pb $(NO_3)_2$, $NiSO_4{\cdot}7H_2O$, and $K_2Cr_2O_7$, respectively, in the distilled water. The experimental solutions of different desired concentrations of metal ions were obtained by diluting the stock solution with the distilled water. The pH of the solution was adjusted using 0.1 M NaOH or 0.1 M HCl.

2.4. Analytical techniques

The concentration of Pb(II), Ni(II), and Cr(VI) ion solution before and after adsorption was measured using an atomic absorption spectrophotometer (AAS) (SL 176 Model, Elico Limited, Chennai, India). To improve the accuracy of the estimating metal ion concentration, the samples were diluted using distilled water whenever it is necessary. The pH of the solution was measured with a pH meter using a combined glass electrode.

2.5. Batch adsorption studies

The adsorption efficiency of the algae biomass (*R. tortuosum*) was examined by conducting the batch adsorption experiment. Adsorption experiments were performed to calculate the percentage removal of Pb (II), Ni(II), and Cr(VI) ions from the aqueous solution by varying the temperature. The pH of the solution was measured with a pH meter using a combined glass electrode and the solution pH was adjusted using 0.1 M HCl or 0.1 M NaOH. In each experiment, the requisite amount of adsorbent (RT) were added into the 100 mL of Pb(II), Ni(II), and Cr(VI) metal ion concentration in the 100 mL of an Erlenmeyer flask and the flasks were placed in a temperature-controlled shaking incubator (25°C) and agitated at 150 rpm with different time intervals. The Pb(II), Ni(II), and Cr(VI) metal ion concentration in the supernatants were calculated using an AAS (SL 176 Model, Elico Limited, Chennai, India). The measured data from the batch adsorption studies were used to calculate the percentage removal of metal ions by using the following formula:

$$\% \text{ Removal of metal ion} = \frac{C_o - C_e}{C_o} \times 100 \quad (1)$$

where C_o and C_e are the initial and final or equilibrium concentrations (mg/L) of metal ions in the solution, respectively.

2.6. Adsorption equilibrium experiments

The adsorption equilibrium experiments were carried out by shaking the solution of desired initial Pb(II), Ni(II), and Cr(VI) metal ion concentrations with

an finest adsorbent dosage in a series of 100 mL Erlenmeyer conical flasks at the pH in the range of 3.0–4.5 for Pb(II) and Ni(II) ions, 2.0–3.5 for Cr(VI) ions at the temperature of 25°C. The conical flasks were shaken in a shaking incubator at an equilibrium contact time. After the equilibrium level was attained, the flasks were withdrawn from the shaking incubator. The metal ion concentration of Pb(II), Ni(II), and Cr(VI) ions in the supernatant was measured using an AAS (SL 176 Model, Elico Limited, Chennai, India). The quantity of metal ions adsorbed onto the biosorbent at equilibrium, q_e (mg/g), was estimated using the following formula:

$$q_e = \frac{(C_o - C_e)V}{m} \tag{2}$$

where q_e is the adsorption capacity at equilibrium (mg/g), V is the volume of metal ions solution (g), C_o is the initial concentration of metal ions (mg/L), C_e is the equilibrium concentration of metal ions (mg/L) in the solution, and m is the biosorbent dosage (g). The two parameter (Langmuir and Freundlich) and three parameter (Redlich–Peterson and Sips) adsorption isotherm models have been used to fit the adsorption equilibrium data. The nonlinear regression analysis was performed to calculate the parameters such as R^2 and error values using MATLAB R2009a software. The adsorption isotherm results provide the information on the design of a batch adsorption system and also to check the types of adsorption process.

2.7. Adsorption kinetic experiments

The adsorption kinetic experiments were performed in a 100-mL Erlenmeyer conical flask. The flask contains 100 mL of metal ion concentration (250–1,000 mg/L) with the finest adsorbent (RT) at different contact time in the range of 5–70 min and the pH in the range of 4.5 for Pb(II) and Ni(II), 2.0 for Cr(VI) ions. The flasks were placed in a temperature-controlled shaking incubator at the temperature of 25°C. After the equilibrium level was attained, the flasks were withdrawn from the shaking incubator. The metal ion concentration Pb(II), Ni(II), and Cr(VI) ions in the supernatant was measured using an AAS (SL 176 Model, Elico Limited, Chennai, India). The amount of metal ions adsorbed onto the adsorbent at different time intervals q_t (mg/g) was calculated using the following formula:

$$q_t = \frac{(C_o - C_t)V}{m} \tag{3}$$

where q_t is the amount of metal ions adsorbed onto the adsorbent at any time t (mg/g), C_o is the initial concentration of metal ions (mg/L), C_t is the concentration of metal ions in the solution measured at time t (mg/L), V is the volume of the metal ions solution (L), and m is the mass of the adsorbent (g).

The adsorption isotherm experimental data were used to determine the rate of adsorption and the rate controlling mechanism of the metal ions removed from aqueous solution. The experimental data were fitted with pseudo-first-order, pseudo-second-order and Elovich kinetic models.

2.8. Thermodynamic study

The adsorption process can be explained by thermodynamic parameters such as Gibbs free energy change (ΔG°, kJ/mol), enthalpy change (ΔH°, kJ/mol), and entropy change (ΔS°, kJ/mol). The thermodynamic parameters can be calculated from the following equations:

$$K_c = \frac{C_{Ae}}{C_e} \tag{4}$$

$$\Delta G^\circ = -RT \ln K_c \tag{5}$$

$$\Delta G^\circ = \Delta H^\circ - T\Delta S^\circ \tag{6}$$

$$\log K_c = \frac{\Delta S^\circ}{2.303\,R} - \frac{\Delta H^\circ}{2.303\,RT} \tag{7}$$

where C_{Ae} is the amount of metal ion adsorbed on the adsorbent per liter of solution at equilibrium (mg/L), C_e is the equilibrium concentration of metal ions in the solution (mg/L), T is the temperature (K), K_c is the equilibrium constant, and R is the gas constant (8.314 J/mol/K). The values of ΔH° and ΔS° were calculated from the slope and the intercept of the plot of $\log K_c$ vs. $1/T$ (Van't Hoff plot).

2.9. Column studies

Continuous flow adsorption experiments were carried out in a glass column. The column was designed with an internal diameter of 3 cm and a height of 30 cm was used for the present adsorption studies. The 1.5 mm diameter of glass beads were placed at the base of the column to reach a height of 2 cm in order to provide the uniform inlet flow of the solutions. A 0.5 mm stainless sieve followed by glass wool was provided at the bottom of the column to support the packing. In the top of the column 0.5 mm stainless

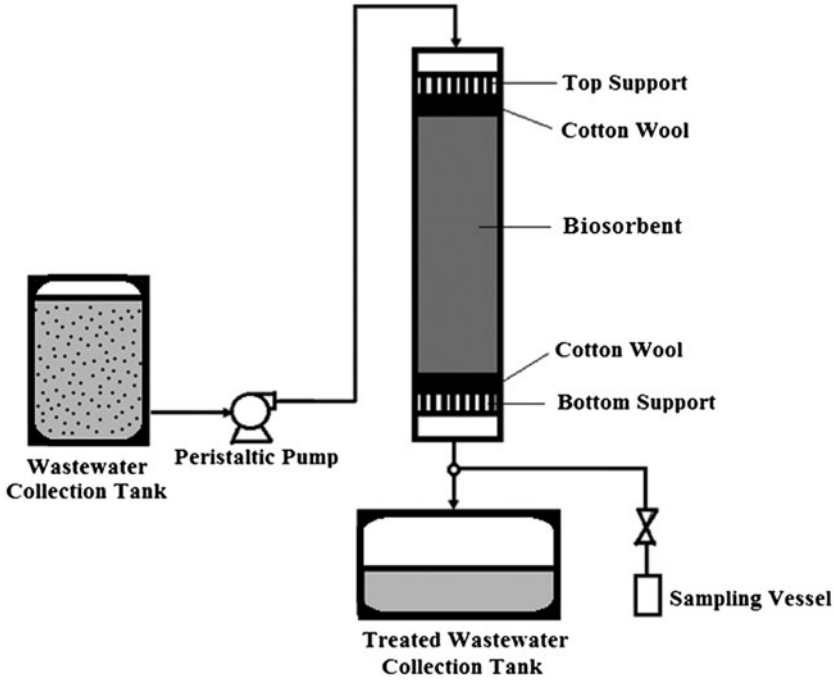

Fig. 1. Schematic diagram of a continuous adsorption column.

sieve of adjustable plunger was placed in order to support the column packing. Fig. 1 shows the schematic diagram of a continuous adsorption column. A known quantity of biosorbent was placed inside the column to attain the desired bed heights. Ni(II) ion solution of known concentration was pumped upward through the column at a desired flow rate by a peristaltic pump (PP40, Miclins). The effluent flow to the column was continued until there was no further adsorption. The samples were collected from the exit of the column at different time intervals. The concentration of Ni(II) ions in the sample was determined using an AAS (SL 176 Model, Elico Limited, Chennai, India).

2.10. Industrial effluent treatment

The untreated raw effluent was collected from plating industry in Chennai, India. The effluent was chosen such that it contains mainly nickel with significant amounts of other heavy and light metals. The pH of the solution was not adjusted, unless otherwise stated. The characteristics of effluent are listed in Table 2. The collected wastewater was treated using the algae biomass—*R. tortuosum* (RT) in a column adsorption experiments.

Table 2
Characteristics of plating industry effluent

Parameters	Units	Values
pH @ 25°C	–	3.34
Conductivity	μS/cm	72,700
Suspended solids	mg/L	1,000
BOD (3 d @ 27°C)	mg/L	268
COD	mg/L	604
Total hardness (as $CaCO_3$)	mg/L	1936
Nickel (as Ni)	mg/L	120
Lead (as Pb)	mg/L	BDL (D.L-0.05)
Copper (as Cu)	mg/L	BDL (D.L-0.1)
Chloride (as Cl)	mg/L	7,395
Iron (as Fe)	mg/L	BDL (D.L-0.1)
Sulfate (as SO_4)	mg/L	27,722
Sodium as Na	mg/L	780
Potassium	mg/L	50

Note: BDL—below detectable limit (detection limit).

3. Results and discussion

3.1. Characterization of R. tortuosum

Algae species—*R. tortuosum* (RT) have been used as the biosorbent for the removal of Pb(II), Ni(II), and Cr(VI) ions from the aqueous solution. The biosorbent was characterized by FTIR and SEM analyzes.

Adsorption process is a surface phenomenon and it is depends on the surface characteristics of the adsorbent. These characteristics study clearly showed that RT has sufficient adsorption capacities for Pb(II), Ni(II), and Cr(VI) metal ions removal from aqueous solutions.

3.2. Fourier transform infrared spectroscopy (FTIR) analysis

The adsorption characteristics of algae species—*R. tortuosum* (RT) fully depends on the chemical reactivity of the functional groups present at the surface. The functional groups such as carboxyl, hydroxyl, and amine groups were capable for adsorbing the metal ions from the aqueous solutions. The FTIR technique was used to identify the various functional groups present on the surface of the adsorbent material (RT) and the interaction between the metal ions and the chemical bounds on the surface of the adsorbent were identified using the FTIR technique. Fig. 2(a) and (b) shows that the FTIR spectroscopy analysis of the *R. tortuosum* (RT) before and after the adsorption. FTIR analysis was carried out using attenuated total reflectance in the range between 450 and 4,000 cm^{-1}. Fig. 2(a) shows the FTIR analysis of algae biomass RT before the adsorption. The intense broad band is observed at 3,401 cm^{-1} is assigned to the O–H carboxylic acid stretching vibration of water and alcohol and the broad band at 1,651.34 and 2,924.87 cm^{-1} is due to N=H amine binding vibrations and alkyl groups, respectively. The broad band at 1,141.26 cm^{-1} could be assigned to the C=H vibration of the alkane's groups.

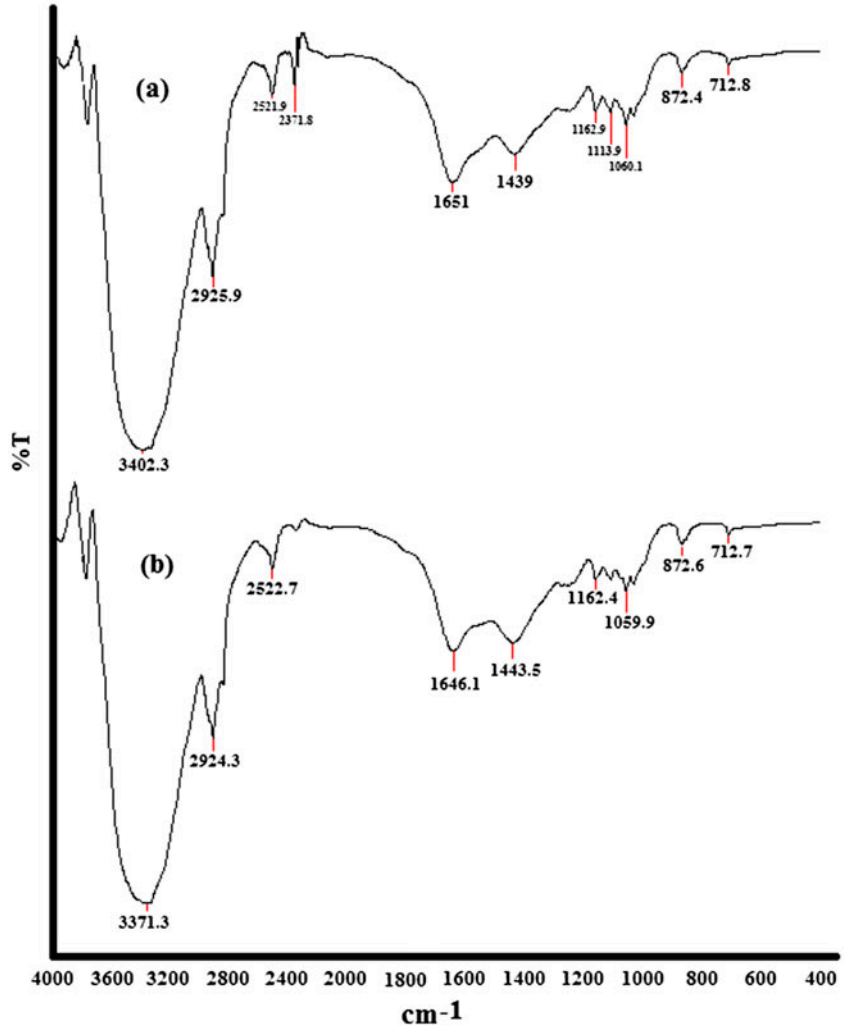

Fig. 2. (a) FT-IR spectrum of before biosorption, (b) after biosorption of Ni(II) ions, (c) SEM image of RT before biosorption, and (d) after biosorption of Ni(II) ions.

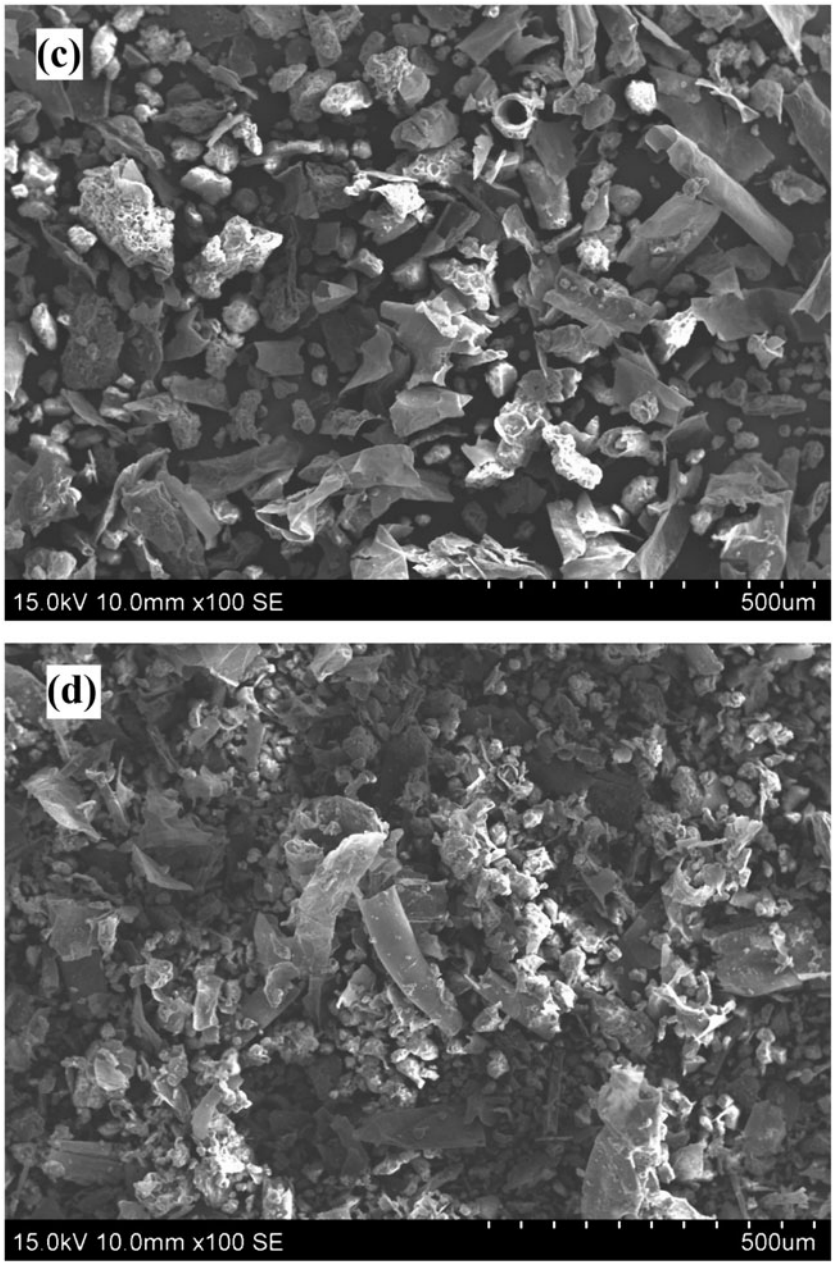

Fig. 2. (*Continued*).

An adsorption peaks at 1,113.06 and 1,059.39 cm^{-1} representing the alcoholic C–O stretching vibration. The broad band is observed at 712.03 cm^{-1} was confirmed that the presence of water in the adsorbents. FTIR analyses showed that the presence of large amounts of water in the RT which indirectly shows the presence of alcoholic and alkyl groups. Fig. 2(b) shows that the Ni(II)-adsorbed algal biomass (RT). The spectrum displayed similar features as shown in Fig. 2(a). However, the carboxylic O–H stretching vibration at 3,402.3 cm^{-1} was shifted to 3,371.3 cm^{-1} indicating that the carboxyl functional group plays a major role for the biosorption over the other functional groups. The above changes after Ni(II) adsorption illustrate that the carboxylate, amino, alkane, alcoholic, and hydroxyl groups were interacted with protons or metal ions. The results confirmed that the algae species (RT) has more potential adsorption capacities for the removal of Ni(II) ions from aqueous solutions.

3.3. SEM analysis

The surface structure and morphology of the adsorbent material were identified using SEM. SEM analysis is an important tool that can be used for illustrate the particle size and porous structure of the adsorbent (RT). Fig. 2(c) and (d) shows the SEM images of algae biomass (RT) before and after Ni(II) ion adsorption. Biosorption mainly depends on the number of pores on the surface of the adsorbents [18]. Large cavities and more pores are the important factors for the absorption of metal ions. Fig. 2(c) clearly shows that more number of pores were available on the surface of the algae biomass. After the adsorption process, the layers were shirked, the surface of the adsorbent materials (pores) were covered by white patches (Ni(II) ions), i.e. the metal ions were adsorbed on the surface of the adsorbent material (RT) from the liquid phase as shown in Fig. 2(d). SEM analyses concluded that the adsorbent material (RT) has more potential for the uptake of Ni(II) ions from the aqueous solutions.

3.4. Effect of biosorbent dose

Batch biosorption studies on effect of adsorbent dose were conducted with RT in different biosorbent dose, from 0.2 to 1.4 g/L in a 100-mL solution containing 100 mg/L of metal ions at pH 4.5 for Pb(II) and Ni(II) ions and pH 2.0 for Cr(VI) ions, for a contact time of 60 min and at 25˚C. The biosorption system was then shaken in a rotary shaker then filtered, and the filtrates were analyzed using the spectrophotometer. The biosorbent dose is an important parameter which helps in the estimation of the amount of biosorbent for the given initial metal ion concentration. The amount of available active sites for the biosorption process depends on the amount of the adsorbent during the adsorption process. The effect of biosorbent dose on the metal uptake and the removal of metal ions were shown in Figs. 3a and 3b, respectively. It was observed that the amount of metal ions adsorbed decreased with an increase in the quantity of dosage. This behavior could be explained by the formation of aggregates of the biomass at higher doses, which decreases the effective surface area for biosorption.

At higher biosorbent dosages, the presence of metal ions is inadequate to cover all the exchangeable sites on the biosorbent which provides fewer uptakes of metal ions onto the biosorbent. Further, it was observed that the percentage removal of metal ions was increased with the increase in biosorbent dosage. The reason for the increase in percentage removal with increase in biosorbent dose was attributed to the

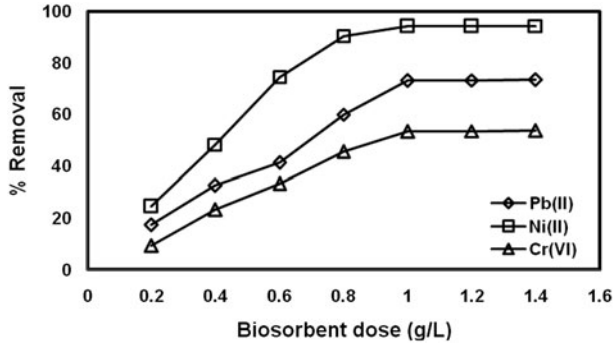

Fig. 3a. Effect of biosorbent dose on the biosorption of metal ions onto RT.

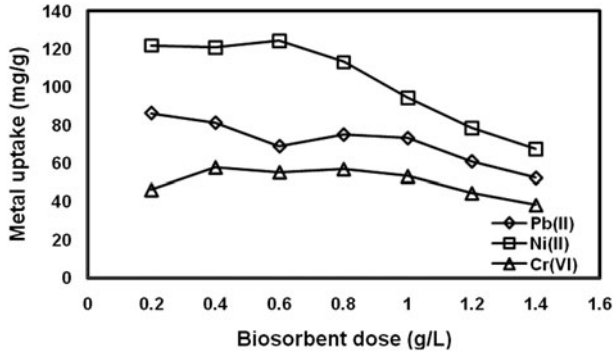

Fig. 3b. Effect of biosorbent dose on the uptake of metal ions onto RT.

increase in the number of available active sites with the increase in adsorbent dose and this reaches a constant value finally which may be due to saturation of the sites. Therefore, 1-g/L dose was selected as the optimum biomass dosage for the present study.

3.5. Effect of temperature and thermodynamic studies

Batch adsorption studies were performed at different temperatures of 25, 30, 35, and 40˚C for Pb(II), Ni (II), and Cr(VI) ions at an optimum conditions to study the adsorption of metal ions from the aqueous solution. Effect of temperature plays an important role for the adsorption process because the mechanism of adsorption process is temperature dependent. Figs. 4a and 4b shows the percentage removal and the metal uptake of Pb(II), Ni(II), and Cr(VI) ions at the pH of 4.5 for Pb(II) and Ni(II) ions, pH of 2.0 for Cr(VI) ions and the biosorbent loading of 1 g/L. The results explored that the percentage and metal uptake of Pb (II), Ni(II), and Cr(VI) ions increased as the temperature increased from 25 to 40˚C. With the increase in

temperature, the pores in the surface of the adsorbent material (RT) have to be increased.

Consequently the availability of active sites were increased for the adsorption, diffusion, and penetration of heavy metals [19] Figs. 4a and 4b stated that the adsorption of metal ions onto the adsorbent materials (RT) is an endothermic process because of the increase in pores in the surface of the algae biomass (RT) or decrease in the layer thickness that surrounds the adsorbents. However, a further increase in the temperature could affects the adsorption process, it was notably indicates that the biosorption is an exothermic process which means adsorption capacity is inversely proportional to the temperature, this might be due to the weakening of adsorptive forces between the active sites and the metal ions on the surface of the adsorbent material [20]. The adsorption process can be explained by thermodynamic parameters such as Gibbs free energy (ΔG°, kJ/mol), enthalpy (ΔH°, kJ/mol), and entropy (ΔS°, kJ/mol). Gibbs free energy (ΔG°) are calculated from Eqs. (11) and (12). The standard enthalpy change (ΔH°) and the standard entropy change (ΔS°) were intended from the slope and the intercept of the linear plot of log K_c vs. $1/T$ (Fig. 4c).

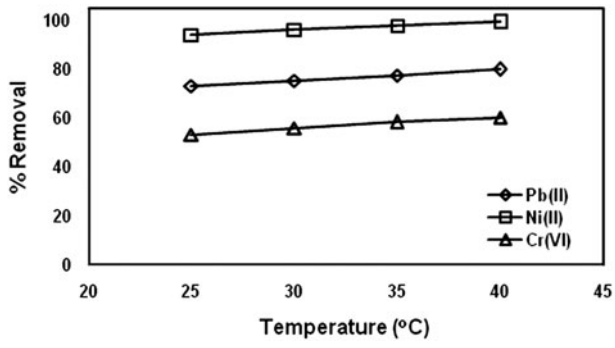

Fig. 4a. Effect of temperature on the removal of metal ions by RT.

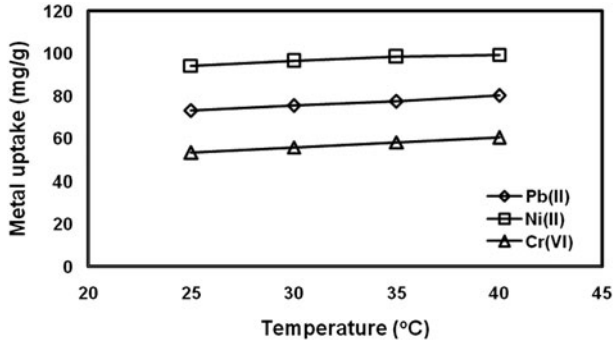

Fig. 4b. Effect of temperature on the biosorption capacity of metal ions onto RT.

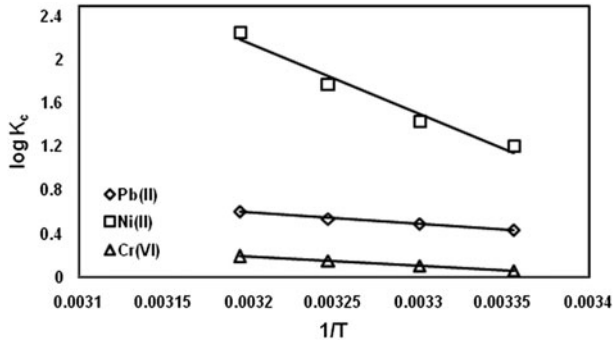

Fig. 4c. Van't Hoff plot for the removal of metal ions by RT.

Table 3 shows the thermodynamic parameters for the adsorption of metal ions onto the adsorbent (RT). The negative value of Gibbs free energy (ΔG°) is increased with an increase in temperature from 25 to 40°C stated that more number of adsorption sites (pores) were available at higher temperature, i.e. the surrounding layers of the adsorbent material is reduced as the temperature increased. The negative value of Gibbs free energy (ΔG°) can conclude that the adsorption of Ni(II) ions onto the adsorbent material (RT) is a spontaneous process [21]. The positive value of standard enthalpy change (ΔH°) indicated that the adsorption of Ni(II) ion onto the algae biomass (RT) is an endothermic process [22]. The positive value of standard entropy change (ΔS°) showed that the adsorption of Ni(II) ions onto the algae biomass (RT) is an enthalpy driven. The thermodynamic parameter studies demonstrated that the algae species—*R. tortuosum* (RT) have more capability for the adsorption of Ni(II) ions from aqueous solution.

3.6. Adsorption kinetic studies

Adsorption kinetics plays a significant role on the design of an adsorption system. The adsorption rates of metal ions from the aqueous solution onto the adsorbents were determined by adsorption kinetic data.

Pseudo-first-order kinetic model [23] equation is given as follows:

$$q_t = q_e(1 - \exp(-k_1 t)) \tag{8}$$

where k_1 is the pseudo-first-order kinetic rate constant (min^{-1}), t is the time (min).

Table 3
Thermodynamic parameters for the adsorption of metal ions onto RT

Metal ions	ΔH° (kJ/mol)	ΔS° (J/mol/K)	ΔG° (kJ/mol)			
			25℃	30℃	35℃	40℃
Pb(II)	20.085	75.689	−4.736	−5.332	−5.940	−6.416
Ni(II)	123.959	436.746	−0.511	−0.749	−0.968	−1.312
Cr(VI)	15.310	52.463	−1.780	−2.156	−2.569	−2.594

Pseudo-second-order kinetic model [24] equation is given as follows:

$$q_t = \frac{q_e^2 k_2 t}{1 + q_e k_2 t} \tag{9}$$

where t is the time (min) and k_2 is the pseudo-second-order kinetic rate constant (g/mg min).

The Elovich kinetic model [25] equation is given as follows:

$$q_t = (1 + \beta_E)\ \ln(1 + \alpha_E \beta_E t) \tag{10}$$

where β_E (g/mg) is the desorption constant related to the activation energy of chemo sorption and α_E is the initial adsorption rate mg/(g min).

The experimental kinetic data provide the useful information to understand the mechanism of the adsorption process. Figs. 5a–5c shows the adsorption kinetic results of Pb(II), Ni(II), and Cr(VI) ions at various initial concentrations (250, 500, 750, and 1,000 mg/L).

Initially, the adsorption rate for all the metal ions will be high because more number of active sites were available at the starting period, which increase the concentration gradient between the metal ions in the solution and the surface of the adsorbent [26]. The equilibrium time was increased with the increase of initial metal ion concentrations, which provide a larger driving force to overcome all mass transfer resistances between the liquid and the solid phase [27]. The adsorption kinetics of metal ions onto the adsorbent

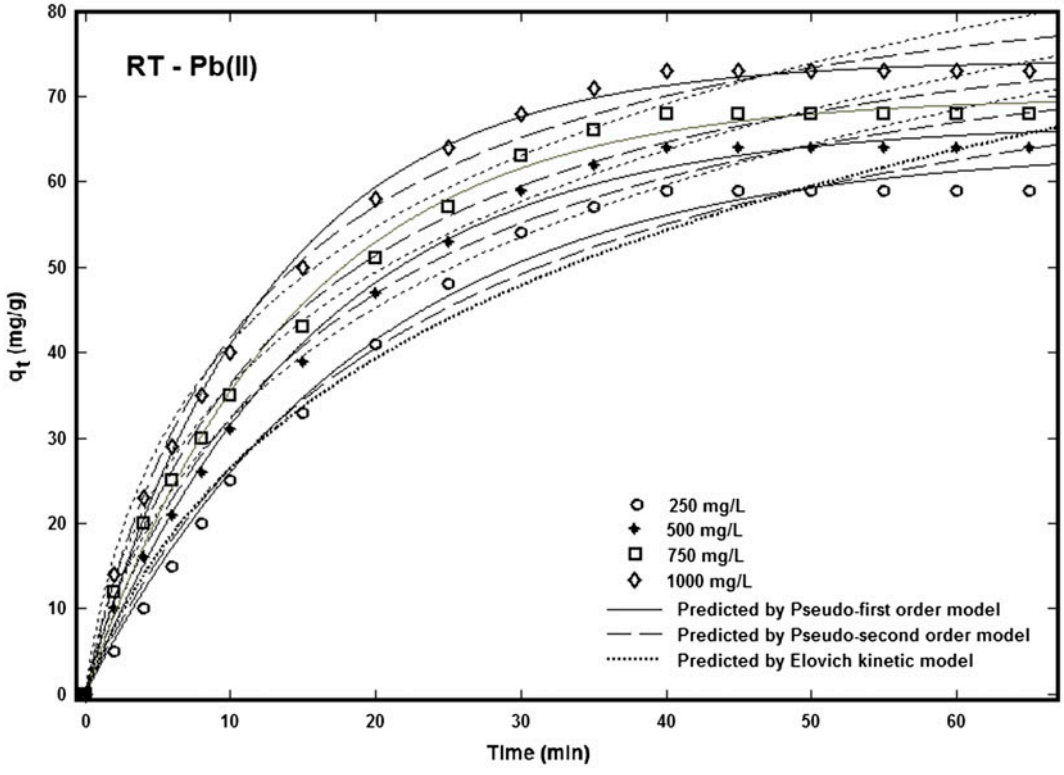

Fig. 5a. Adsorption kinetic model fits for removal of Pb(II) ions by RT.

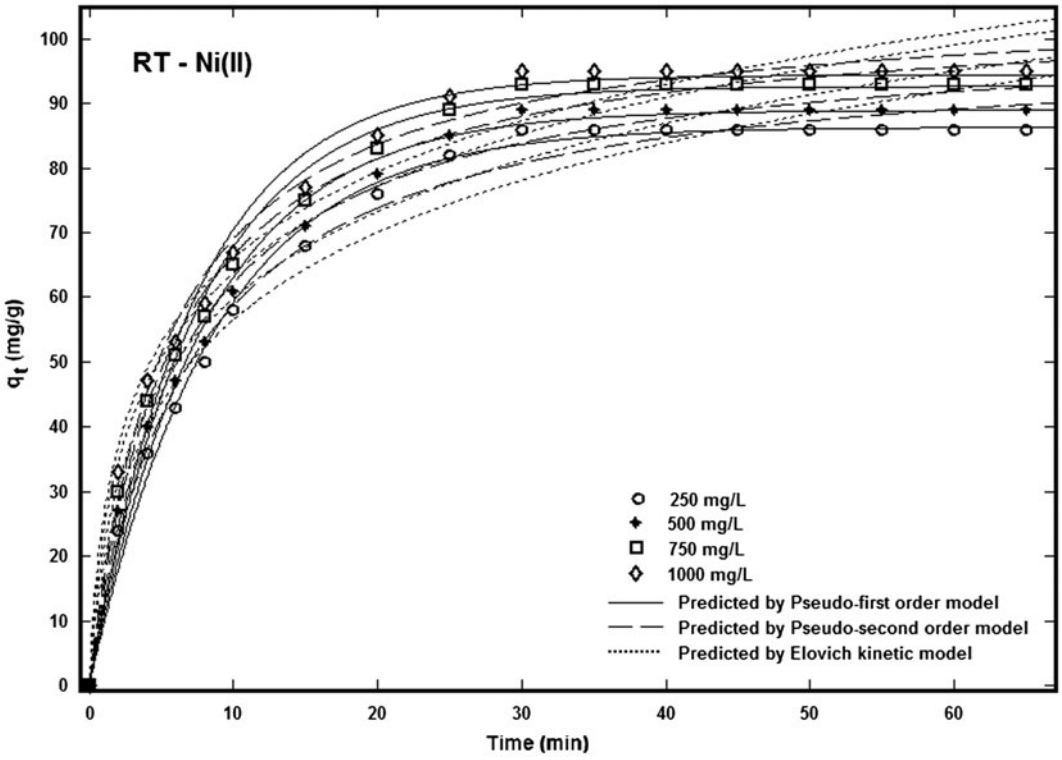

Fig. 5b. Adsorption kinetic model fits for removal of Ni(II) ions by RT.

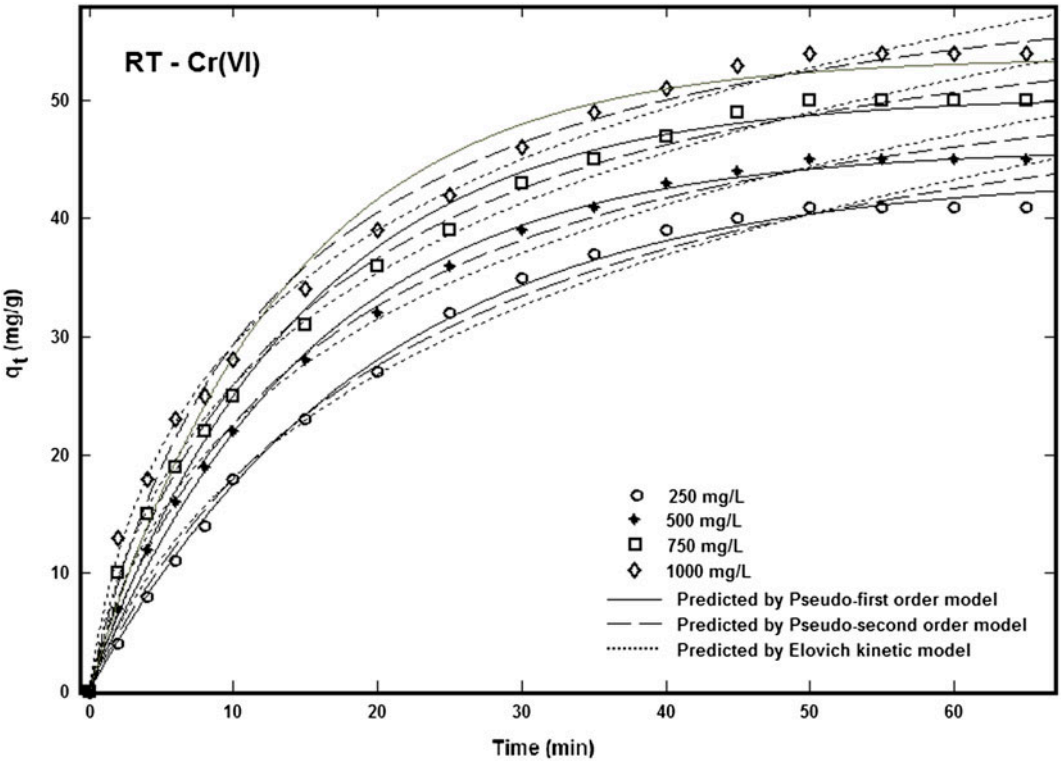

Fig. 5c. Adsorption kinetic model fits for removal of Cr(VI) ions by RT.

material (RT) was carried out using pseudo-first-order, pseudo-second-order and Elovich kinetic models. The pseudo-first-order kinetics constant (k_1) and q_e, the pseudo-second-order kinetic constant (k_2) and q_e, the Elovich kinetic model constant (α_E) and β_E and the parameters such as correlation coefficient values (R^2) and error values (sum of squared errors (SSE), root mean squared values (RMSE)) were determined by nonlinear regression analysis, using a MATLAB R2009a software. Tables 4a–4c shows the predicted kinetic parameter data for the Pb(II), Ni(II) and Cr(VI) metal ions.

The experimental results were used to identify the best-fitted adsorption kinetic model. The calculated adsorption capacity ($q_{e,cal}$) values were compared with the experimental equilibrium adsorption capacity ($q_{e,exp}$) values of pseudo-first-order, pseudo-second-order, and Elovich kinetic model of the algae biomass (RT). The comparison statement clearly confirmed that the calculated adsorption capacity ($q_{e,cal}$) values of the pseudo-second-order kinetic model were closer to the experimental adsorption capacity ($q_{e,exp}$) values. The correlation coefficient values (0.9913, 0.9958, 0.995, and 0.9969 at 250, 500, 750, and 100 mg/L, respectively, for Pb(II) ions and 0.993, 0.9905, 0.9911, and 0.9901 at 250, 500, 750, and 100 mg/L, respectively, for Ni(II) ions and 0.998, 0.9971, 0.9958, and 0.9912 at 250, 500, 750, and 100 mg/L, respectively, for Cr(II) ions) for the pseudo-second-order kinetics were superior than the pseudo-first-order kinetic and Elovich kinetic models. The pseudo-second-order kinetic data stated that the adsorption process involves chemisorption mechanism and the rate of site occupation is proportional to the square of the number of unoccupied sites. This result indicated that the pseudo-second-order kinetic is the best-fitted adsorption kinetic model for the adsorption of Pb(II), Ni(II), and Cr(VI) ions from the aqueous solution onto the adsorbents.

3.7. Effect of pH and adsorption isotherm studies

The initial metal ion concentration plays a significant role in the adsorption of metal ions onto the algae biomass (RT). The initial concentration of Pb(II), Ni(II), and Cr(VI) ions solutions were ranged from 250 to 1,000 mg/L. The isotherm experimental data (q_e and C_e) were fitted to the following adsorption isotherm models such as two-parameter equations (Langmuir and Freundlich equation) and three-parameter equations (Redlich–Peterson and Sips model).

Langmuir [28] adsorption isotherm model equation is given by:

$$q_e = \frac{q_m K_L C_e}{1 + K_L C_e} \tag{11}$$

where q_e is the adsorption capacity at equilibrium (mg/g), q_m is the maximum monolayer adsorption capacity (mg/g), K_L is the Langmuir equilibrium

Table 4a
Kinetic parameters for the adsorption of Pb(II) ions onto RT

		Concentration of Pb(II) ion solution (mg/L)			
Kinetic model	Parameters	250	500	750	1,000
Pseudo-first-order equation	k_1 (min^{-1})	0.05221	0.06376	0.07067	0.0804
	$q_{e,cal}$ (mg/g)	85.88	85.23	87.14	90.5
	R^2	0.9812	0.9888	0.9909	0.9927
	SSE	145.4	88.81	77.16	69.01
	RMSE	3.113	2.433	2.268	2.145
Pseudo-second-order equation	k_2 (g/mg min)	0.00052	0.0007174	0.0008234	0.0009469
	$q_{e,cal}$ (mg/g)	64.01	66.88	69.99	74.25
	$q_{e,exp}$ (mg/g)	59.35	64.49	68.82	73.62
	R^2	**0.9913**	**0.9958**	**0.995**	**0.9969**
	SSE	67.53	33.7	42.74	29.43
	RMSE	2.122	1.499	1.688	1.401
Elovich kinetic equation	α (mg/g min)	0.01711	0.03319	0.04558	0.06228
	β (g/mg)	10.3	9.079	8.769	8.639
	R^2	0.9691	0.9772	0.9801	0.9789
	SSE	238.9	181.2	168.3	197.8
	RMSE	3.991	3.476	3.349	3.632

Note: The bold values indicate that the given model is a best obeyed model for the present adsorption system.

Table 4b
Kinetic parameters for the adsorption of Ni(II) ions onto RT

		Concentration of Ni(II) ion solution (mg/L)			
Kinetic model	Parameters	250	500	750	1,000
Pseudo-first-order equation	k_1 (min^{-1})	0.1159	0.1237	0.1314	0.1372
	$q_{e,cal}$ (mg/g)	99.41	101.5	104.9	106.2
	R^2	0.9899	0.9892	0.9864	0.9813
	SSE	115.8	126.8	169	234.6
	RMSE	2.779	2.907	3.357	3.955
Pseudo-second-order equation	k_2 (g/mg min)	0.00145	0.001567	0.001655	0.001748
	$q_{e,cal}$ (mg/g)	88.32	91.95	95.65	98.4
	$q_{e,exp}$ (mg/g)	86.45	89.18	93.23	95.17
	R^2	**0.993**	**0.9905**	**0.9911**	**0.9901**
	SSE	80.55	111	110.4	124.7
	RMSE	2.317	2.72	2.713	2.883
Elovich kinetic equation	α (mg/g min)	0.1876	0.2396	0.2941	0.3558
	β (g/mg)	7.891	7.738	7.736	7.601
	R^2	0.9677	0.9704	0.9719	0.9735
	SSE	368.6	347.3	347.7	331.7
	RMSE	4.957	4.812	4.815	4.703

Note: The bold values indicate that the given model is a best obeyed model for the present adsorption system.

Table 4c
Kinetic parameters for the adsorption of Cr(VI) ions onto RT

		Concentration of Cr(VI) ion solution (mg/L)			
Kinetic model	Parameters	250	500	750	1,000
Pseudo-first-order equation	k_1 (min^{-1})	0.05111	0.06486	0.06846	0.0747
	$q_{e,cal}$ (mg/g)	58.48	58.1	62.68	65.44
	R^2	0.9931	0.9971	0.9904	0.9791
	SSE	23.69	10.52	40.18	96.09
	RMSE	1.257	0.8375	1.637	2.531
Pseudo-second-order equation	k_2 (g/mg min)	0.0007605	0.001099	0.001123	0.001242
	$q_{e,cal}$ (mg/g)	43.78	46.99	52.4	57.69
	$q_{e,exp}$ (mg/g)	41.22	45.18	50.06	54.12
	R^2	**0.998**	**0.9971**	**0.9958**	**0.9912**
	SSE	6.82	10.44	17.48	40.59
	RMSE	0.6743	0.8344	1.079	1.645
Elovich kinetic equation	α (mg/g min)	0.02734	0.05745	0.06713	0.08975
	β (g/mg)	6.608	5.74	5.982	5.912
	R^2	0.9852	0.9906	0.9936	0.9938
	SSE	50.54	34.36	26.87	28.56
	RMSE	1.836	1.514	1.338	1.38

Note: The bold values indicate that the given model is a best obeyed model for the present adsorption system.

constant related to the affinity of metal ions to the biosorbent (L/mg), and C_e is the concentration of the metal ions in the solution at equilibrium (mg/L).

Freundlich [29] adsorption isotherm model equation is given by:

$$q_e = K_F C_e^{1/n} \tag{12}$$

where K_F is the Freundlich constant [(mg/g) $(L/mg)^{(1/n)}$] related to the bonding energy and n is

the measure of the deviation from the linearity of adsorption (g/L). The significance of "n" is as follows: $n = 1$ (linear); $n < 1$ (chemical process); $n > 1$ (physical process).

The Redlich–Peterson [30] adsorption isotherm model equation is given by:

$$q_e = \left(\frac{K_{RP} C_e}{1 + a_{RP} C_e^{\beta_{RP}}}\right) \tag{13}$$

where K_{RP} is Redlich–Peterson isotherm constant (L/g), a_{RP} is Redlich–Peterson isotherm constant $(L/mg)^{1/\beta_{RP}}$ and β_{RP} is the exponent which lies between 0 and 1. The significance of "β" is as follows: $\beta = 1$ (Langmuir adsorption isotherm model is a preferable adsorption isotherm model); $\beta = 0$ (Freundlich adsorption isotherm model is a preferable adsorption isotherm model).

Sips [31] adsorption isotherm model equation is given by:

$$q_e = \left(\frac{K_S C_e^{\beta_S}}{1 + a_S C_e^{1/\beta_S}}\right) \tag{14}$$

where K_S is the Sips model isotherm constant $(L/g)^{\beta_S}$, a_S is the Sips model constant $(L/g)^{1/\beta_S}$ and β_S is the Sips model exponent. The constant β_S is often regarded as the heterogeneity factor, with values greater than 1 indicating a heterogeneous adsorption system. Values close to (or exactly) 1 indicate that the material has relatively homogenous binding sites. For $\beta_S = 1$, the Sips model reduces to the Langmuir equation.

The interaction behavior between the adsorbent material (RT) and the solutes can be explained by the above isotherm models. These isotherm models were applied to examine the effect of initial metal ion concentration at different pH in the range of 3.0–4.5 for Pb(II) and Ni(II) ions, pH 2.0–3.5 for Cr(VI) ions and the results are shown in Figs. 6a–6f. The pH of the solution plays an important role in the adsorption of metal ions from aqueous solutions. Pb(II), Ni(II), and Cr(VI) ions is to be present as ionic form in the aqueous solutions. pH values changes the ionization state of functional groups such as amino, carboxyl and phosphate groups present at the cell walls and affect the chemical speciation of metal ions [32].

The percentage removal of Pb(II) and Ni(II) ions is increased with an increase in the pH range of 3.0–4.5, similarly for Cr(VI) ions in the pH range of 2.0–3.5, which clearly stated that the rate of adsorption capacity is increased under acidic condition. At acidic condition, the surface of the adsorbent to be positively charged, which attracts the negatively charged metal ions because of the electrostatic force of attraction [33]. Beyond the pH range of 4.5, the percentage removal of Pb(II) and Ni(II) ions is gradually decreased, similarly beyond the pH of 3.5, the percentage removal of Cr(VI) ions is gradually decreased because of the presence of hydroxyl ions which causes the formation of metal hydroxide complexes, which decrease the adsorption capacity of adsorbent material (RT). From the results the maximum percentage removal of Pb(II), Ni(II), and Cr(VI) ions from aqueous solutions was found to be at pH 4.5 and 3.5, respectively. The experimental values q_e and C_e are primarily treated with the adsorption isotherm models, the adsorption isotherm data are shown in Tables 5a–5c.

3.7.1. Two and three parameter adsorption isotherm models

Two parameter adsorption isotherm model (Langmuir and Freundlich) were used to investigate the adsorption rate of Pb(II), Ni(II), and Cr(VI) ions onto the adsorbent material (RT). Figs. 6a, 6c and 6e shows that the two parameter isotherm model was very fitting for the adsorbents. Figs. 6b, 6d and 6f shows that the three parameter isotherm model was very fitting for the adsorbents. The parameters of these models such as the Langmuir maximum adsorption capacity (q_m) and the equilibrium constant (K_L), the Freundlich equilibrium constant (K_F), the Redlich–Peterson equilibrium constant (K_{RP}) and the Sips equilibrium constant (K_S) and the correlation coefficient values (R^2), and error values (SSE and RMSE) were examined by nonlinear regression analysis, using a MATLAB R2009a software. Best-fitted adsorption isotherm model were identified using the correlation coefficient values (R^2). The Sips model shows that the higher correlation coefficient values (0.9816, 0.9914, 0.9914, 0.9956 and 0.9828, 0.9733, 0.9863, 0.983, and 0.9982, 0.9975, 0.9989, 0.9988 at the metal ion concentration of 250, 500, 750, and 100 mg/L for Pb(II), Ni(II), and Cr(VI) ions, respectively) and the lower error values (SSE = 83.06, 38.43, 35.39, 24.31, and 143.1, 235.8, 136.6, 167.1 and 6.87, 8.245, 2.975, 2.792 at the metal ion concentration of 250, 500, 750, 100 mg/L for Pb(II), Ni(II) and Cr(VI) ions, respectively) RMSE = 2.882, 1.96, 1.881, 1.559 and 3.783, 4.856, 3.696, 4.088 and 0.8288, 0.908, 0.5454, 0.5006 at the metal ion concentration of 250, 500, 750, 100 mg/L for Pb(II), Ni(II) and Cr(VI) ions, respectively). Tables 5a–5c clearly demonstrate that the experimental isotherm data are well depicted, from that values three parame-

Table 5a
Isotherm constants of two-parameters and three-parameters models for the removal of Pb(II) ions by the RT

Adsorption isotherm models	pH	3.0	3.5	4.0	4.5
Two-parameters model constants					
Langmuir	q_m (mg/g)	60.15	59.65	57.22	66.08
	K_L (L/mg)	0.01629	0.02235	0.03656	0.03154
	R^2	0.9588	0.9587	0.9427	0.9047
	SSE	186	183.7	236.2	528.1
	RMSE	4.113	4.087	4.634	6.929
Freundlich	K_F ((mg/g) (L/mg)$^{(1/n)}$))	7.308	9.548	12.86	14.05
	n	3.105	3.522	4.225	4.097
	R^2	0.9732	0.9851	0.9864	0.9956
	SSE	120.9	66.35	55.89	24.3
	RMSE	3.315	2.456	2.254	1.486
Three-parameters model constants					
Redlich–Peterson	K_{RP} (L/g)	2.348	4.317	9.389	1.256
	a_{RP} (L/mg)$^{(1/\beta_{RP})}$)	0.1604	0.2867	0.5527	0.1012
	β_{RP}	0.7823	0.7856	0.8068	0.7565
	R^2	0.9808	0.9908	0.9909	0.9956
	SSE	86.76	40.93	37.39	24.34
	RMSE	2.946	2.023	1.934	1.56
Sips	K_S (L/g)$^{\beta_S}$	1.801	3.438	7.86	0.728
	a_S (L/mg)$^{(\beta_S)}$	0.1363	0.2429	0.4762	0.0835
	β_S	1.122	1.117	1.103	1.129
	R^2	0.9816	0.9914	0.9914	0.9956
	SSE	83.06	38.43	35.39	24.31
	RMSE	2.882	1.96	1.881	1.559

ter Sips adsorption isotherm model better than the other parameter model: Langmuir, Freundlich, and Redlich–Peterson. Sips adsorption isotherm model markedly stated that the adsorbent material (RT) surface is heterogeneity. The results strongly reported that the adsorbent surface is made up of heterogeneous patches which are very constructive for adsorption process. The Langmuir monolayer capacity (q_m) of the RT for the elimination of metal ions was compared with the other low-cost adsorbents. The comparison details were presented in Table 5d. The results indicate that the highest value of Langmuir monolayer capacity of RT was observed as compared with the other cheap adsorbents.

3.8. Column adsorption studies

The adsorption efficiency of adsorbent material and its behavior were studied using the batch experimental results. However, the batch adsorption experiment data could not give the scale-up data for industrial treatment systems, whereas continuous flow system (column) studies were normally employed for scale-up process [47]. Column adsorption studies are an effective process for metal adsorption. From the beginning, at the inlet the saturated solid sorbent zones slowly widen throughout the column and then the adsorbent material is breaking throughout the column. The record of breakthrough gives usually a typical S-shaped breakthrough curve whose shape and slope is mainly the result of the equilibrium sorption isotherm. In the column experiment study, relatively low initial metal concentration (100 mg/L) was used because low concentrations of metals were present in industrial effluents. In the present study, the adsorption competence of RT increases in the following series nickel > lead > chromium. Therefore, nickel was selected as the model metal ions for investigate the performance of RT on continuous removal.

3.8.1. Effect of bed height

The adsorption capacity of adsorbent material (RT) was tested using diverse bed heights (20, 25, 30 cm) at the different flow rate (10, 15, 20 mL/min) and different initial Ni(II) ions concentration (50, 75, 100 mg/L).

Table 5b
Isotherm constants of two-parameters and three-parameters models for the removal of Ni(II) ions by the RT

Adsorption isotherm models	pH	3.0	3.5	4.0	4.5
Two-parameters model constants					
Langmuir	q_m (mg/g)	79.04	80.46	85.09	84.25
	K_L (L/mg)	0.02069	0.03383	0.03921	0.06392
	R^2	0.976	0.968	0.9743	0.9669
	SSE	199.2	282.9	255.7	326.1
	RMSE	4.256	5.072	4.821	5.445
Freundlich	K_F ((mg/g) (L/mg)$^{(1/n)}$))	11.09	16.06	18.12	23.08
	n	3.292	3.935	4.063	4.759
	R^2	0.9552	0.9365	0.9581	0.9536
	SSE	372.4	560.9	416.7	456.4
	RMSE	5.819	7.141	6.155	6.442
Three-parameters model constants					
Redlich–Peterson	K_{RP} (L/g)	2.195	3.421	5.074	8.783
	a_{RP} (L/mg)$^{(1/\beta_{RP})}$	0.0545	0.06665	0.1152	0.19
	β_{RP}	0.8939	0.9277	0.8937	0.9013
	R^2	0.9817	0.9723	0.9854	0.9822
	SSE	152	245.1	145.8	175.5
	RMSE	3.898	4.95	3.819	4.189
Sips	K_S (L/g)$^{\beta_S}$	1.93	3.182	4.592	8.164
	a_S (L/mg)$^{(\beta_S)}$	0.05468	0.06778	0.1122	0.1852
	β_S	1.064	1.044	1.06	1.054
	R^2	0.9828	0.9733	0.9863	0.983
	SSE	143.1	235.8	136.6	167.1
	RMSE	3.783	4.856	3.696	4.088

The adsorption of metal ions in the continuous flow system highly depends on the bed height of *R. tortuosum* (RT) in the column. The effect of bed height on the adsorption capacity of the algae biomass (RT) for metal ions at pH 4.5, 100 mg/L of Ni(II) ions solution, 10 mL/min of flow rate, and at constant temperature of 25˚C was determined. In order to yield different bed heights 6.25, 8.3, and 9.8 g of algae biomass (RT) were added to the column to attain the bed heights of 20, 25, and 30 cm, respectively. Fig. 7a shows the effect of bed height on the removal of Ni(II) ions using adsorbent material (RT).

Table 6 shows the column data and their parameters obtained at different bed heights onto the adsorbent (RT) which clearly stated that the both breakthrough and exhaustion time increases as the bed height increases because of the increase in the surface area of the adsorbent material (RT). The slope of the S-curve from t_b to t_e is decreases as the bed height increased from 20 to 30 cm indicating that the breakthrough curve becomes steeper as the bed height decreases. The adsorption competence of the algae biomass (RT) remained relatively constant for different bed height. Even though, to some extent high biosorption capacities were observed at the highest bed height (30 cm). In the column with the increased bed height could be useful to treat high volume of metal ion solution and also the percentage removal of metal ions could be higher.

3.8.2. Effect of flow rate

Flow rate plays an important role for the estimation of adsorption capacity of adsorbent material in the continuous treatment of wastewater on industrial level. The effect of different flow rates (10, 15, 20 mL/min) on the sorption of Ni(II) ions using *R. tortuosum* (RT) at optimum bed height (30 cm) and 100 mg/L initial Ni(II) ion concentration at constant temperature of 25˚C in column was investigated. Fig. 7b shows the effect of flow rate on the removal of Ni(II) ions using adsorbent material (RT). Table 6 shows the column data and their parameters obtained at different flow rate onto the adsorbent (RT) which clearly stated that the both breakthrough and exhaustion time decreases as the bed height increases

Table 5c
Isotherm constants of two-parameters and three-parameters models for the removal of Cr(VI) ions by the RT

Adsorption isotherm models	pH	2.0	2.5	3.0	3.5
Two-parameters model constants					
Langmuir	q_m (mg/g)	58.96	61.45	51.41	60.42
	K_L (L/mg)	0.00713	0.00425	0.00471	0.00203
	R^2	0.9874	0.9937	0.9909	0.9987
	SSE	45.9	20.71	21.87	2.792
	RMSE	2.043	1.372	1.41	0.5038
Freundlich	K_F ((mg/g) (L/mg)$^{(1/n)}$))	3.36	1.847	1.778	0.5689
	n	2.389	2.009	2.082	1.574
	R^2	0.9938	0.9934	0.996	0.9906
	SSE	22.61	21.85	9.678	20.06
	RMSE	1.434	1.409	0.938	1.351
Three-parameters model constants					
Redlich–Peterson	K_{RP} (L/g)	0.9806	0.4402	0.5487	0.1215
	a_{RP} (L/mg)$^{(1/\beta_{RP})}$	0.1141	0.04817	0.106	0.00203
	β_{RP}	0.7159	0.7244	0.6682	0.9982
	R^2	0.9981	0.9975	0.9988	0.9987
	SSE	7.336	10.05	3.393	2.506
	RMSE	0.8565	1.003	0.5825	0.5038
Sips	K_S (L/g)$^{\beta_S}$	0.7024	0.2933	0.3658	0.1772
	a_S (L/mg)$^{(\beta_S)}$	0.1072	0.05578	0.1045	0.00055
	β_S	1.172	1.188	1.208	0.8991
	R^2	0.9982	0.9975	0.9989	0.9988
	SSE	6.87	8.245	2.975	2.792
	RMSE	0.8288	0.908	0.5454	0.5006

because the adsorption competence of the adsorbent material is decreased with the increasing flow rate in column operations. The reason for this behavior can be explained in two ways: (1) when the flow rate increases the residence time of the solute in the column decreases which causes the metal solution to leave the column before equilibrium occurs, (2) when the process is intra particle, mass transfer controlled a slower flow rate favors the sorption and when the process is subjected to external mass transfer control a higher flow rate decreases the film resistance. Also the lowest flow rate (10 mL/min) displayed a relatively high percentage removal of Ni(II) ions.

3.8.3. Effect of Ni(II) ion concentration

The effect of initial Ni(II) ion concentration (50, 75, 100 mg/L) on the sorption of Ni(II) ions using *R. tortuosum* (RT) at optimum bed height (30 cm) and optimum flow rate (10 mL/min) at constant temperature of 25˚C in column was investigated. Fig. 7c shows the effect of initial Ni(II) ion concentration on the removal of Ni(II) ions by using adsorbent material (RT). Table 6 shows the column data and their parameters obtained at different Ni(II) ion concentration onto the adsorbent (RT). At the lower Ni(II) ion concentration, the percentage removal is low due to the delayed breakthrough curves, lower concentration gradient, and slower transport of adsorbents [48]. At the higher Ni (II) ions concentration (100 mg/L) the adsorbent material *R. tortuosum* (RT) saturated quickly leading to earlier breakthrough and exhaustion time. However, the higher adsorption of metal ions were attained at the Ni(II) ions concentration of 100 mg/L. Thus, the results stated that the higher Ni(II) ion concentration (100 mg/L) provide a larger driving force to overcome all mass transfer resistances between the liquid and the solid phase which shows the better performance for adsorption in the column study.

3.8.4. Bed depth service time model

The adsorption capacity of the bed at different breakthrough values was measured using the bed

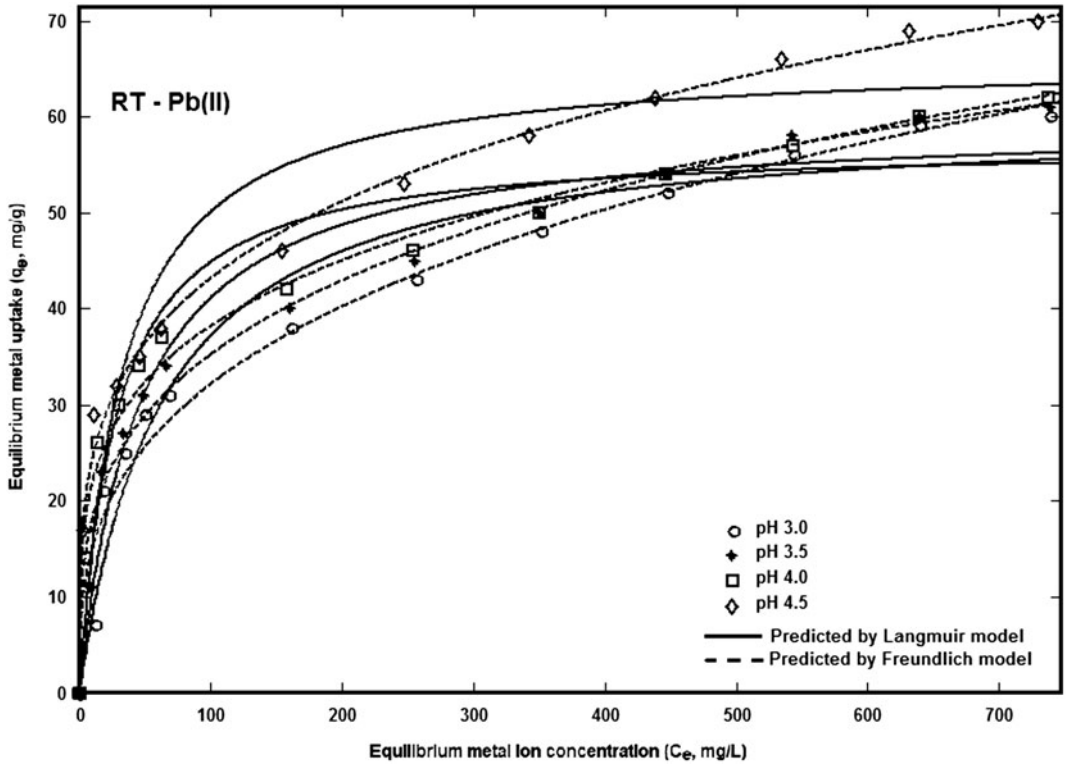

Fig. 6a. Adsorption isotherm model (2 parameter) fits for removal of Pb(II) ions by RT.

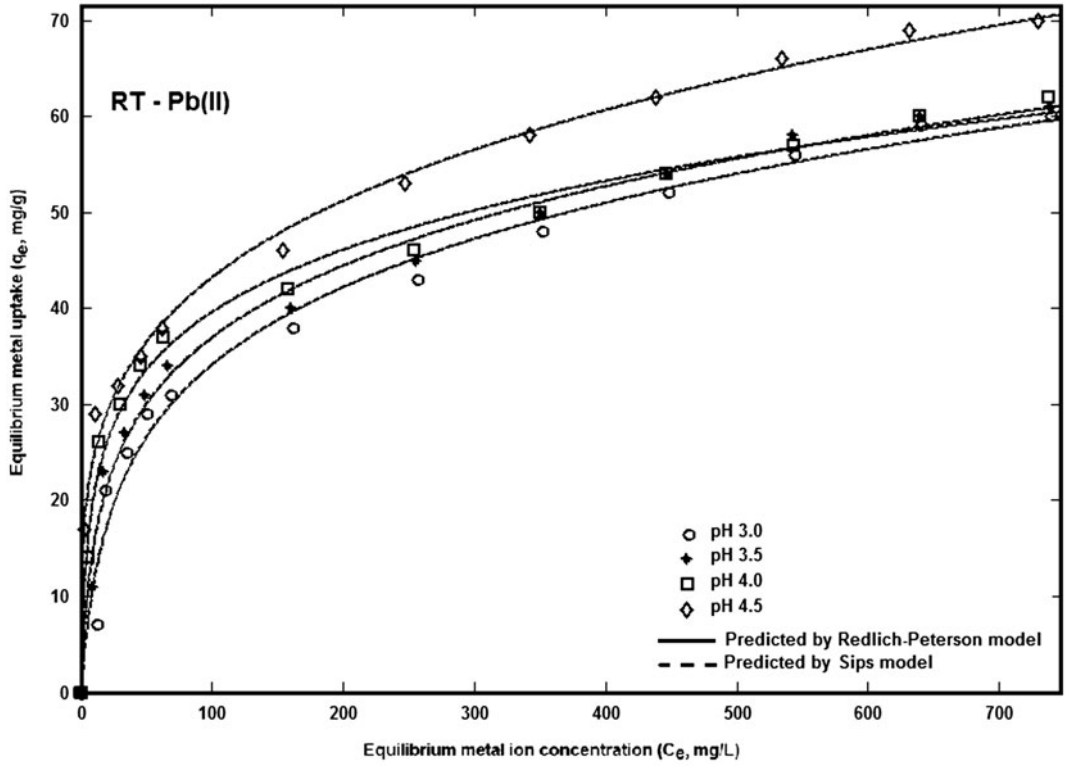

Fig. 6b. Adsorption isotherm model (3 parameter) fits for removal of Pb(II) ions by RT.

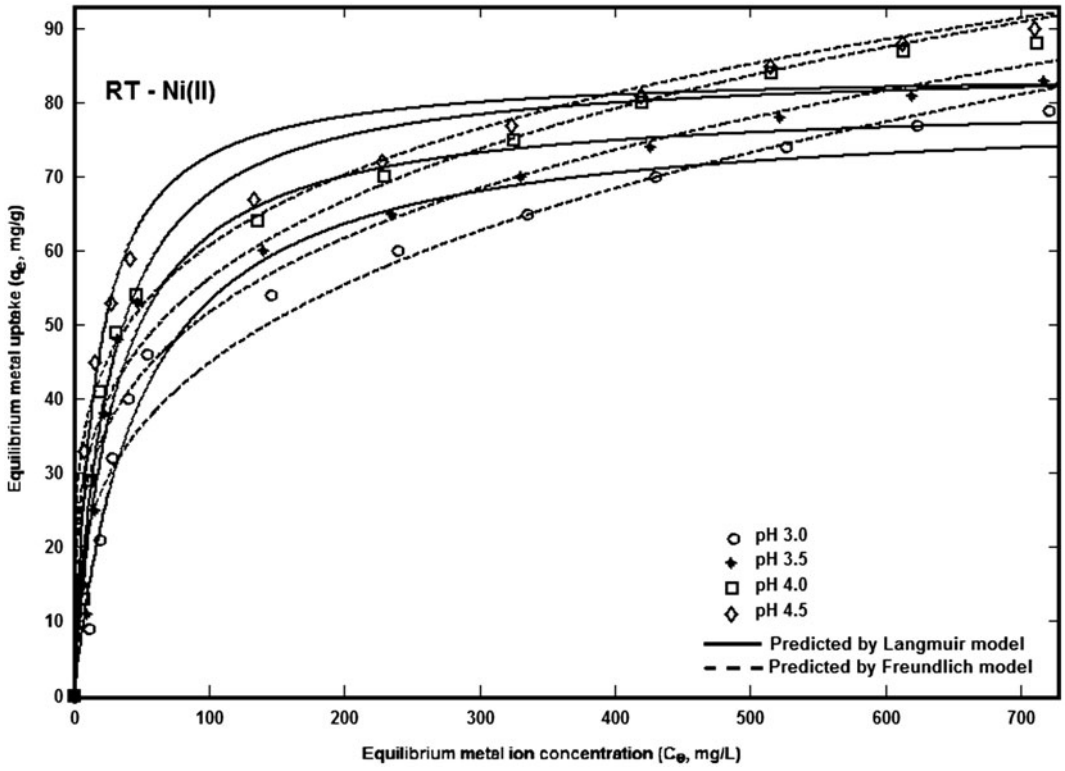

Fig. 6c. Adsorption isotherm model (2 parameter) fits for removal of Ni(II) ions by RT.

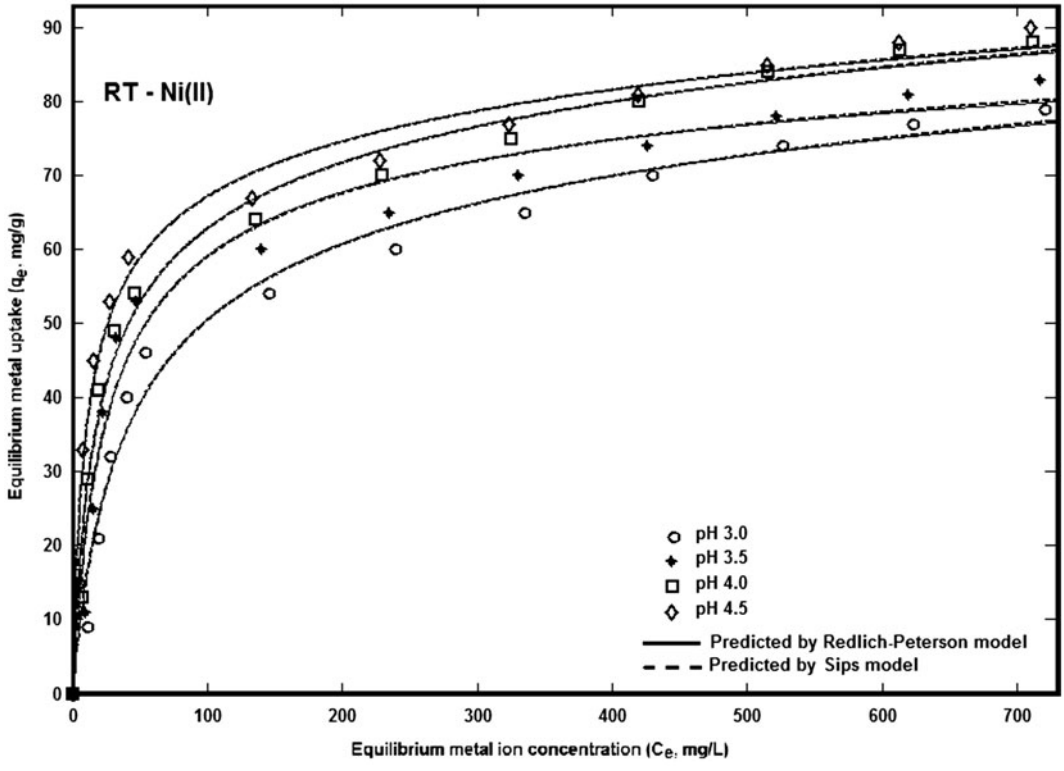

Fig. 6d. Adsorption isotherm model (3 parameter) fits for removal of Ni(II) ions by RT.

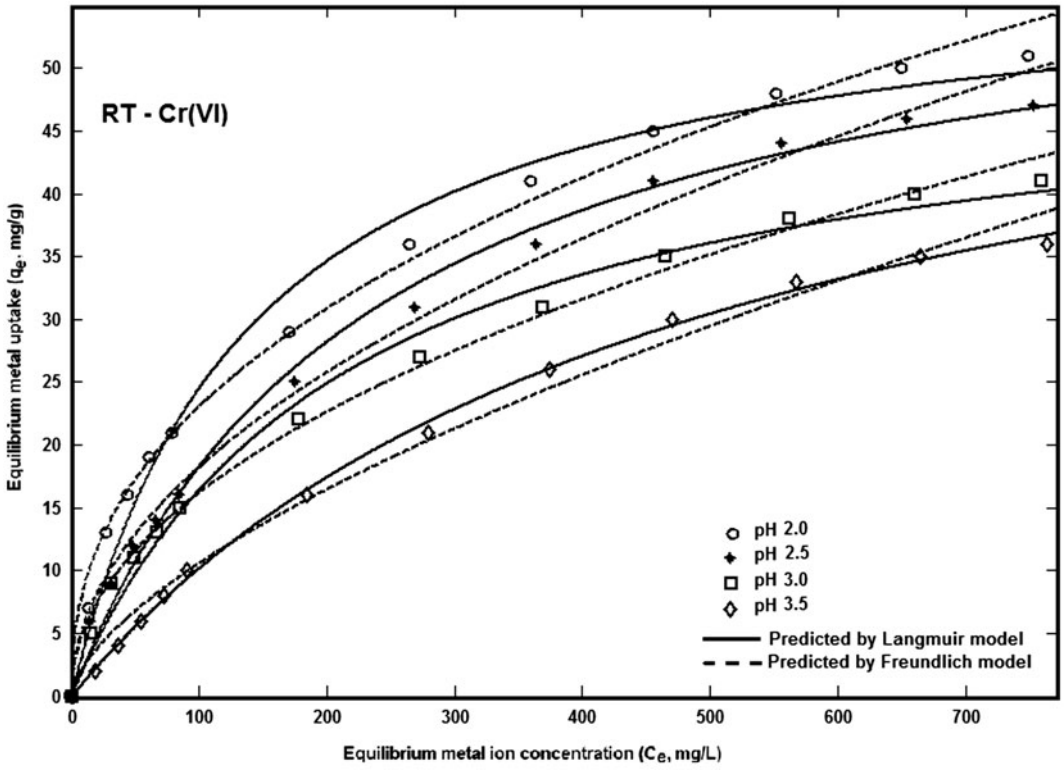

Fig. 6e. Adsorption isotherm model (2 parameter) fits for removal of Cr(VI) ions by RT.

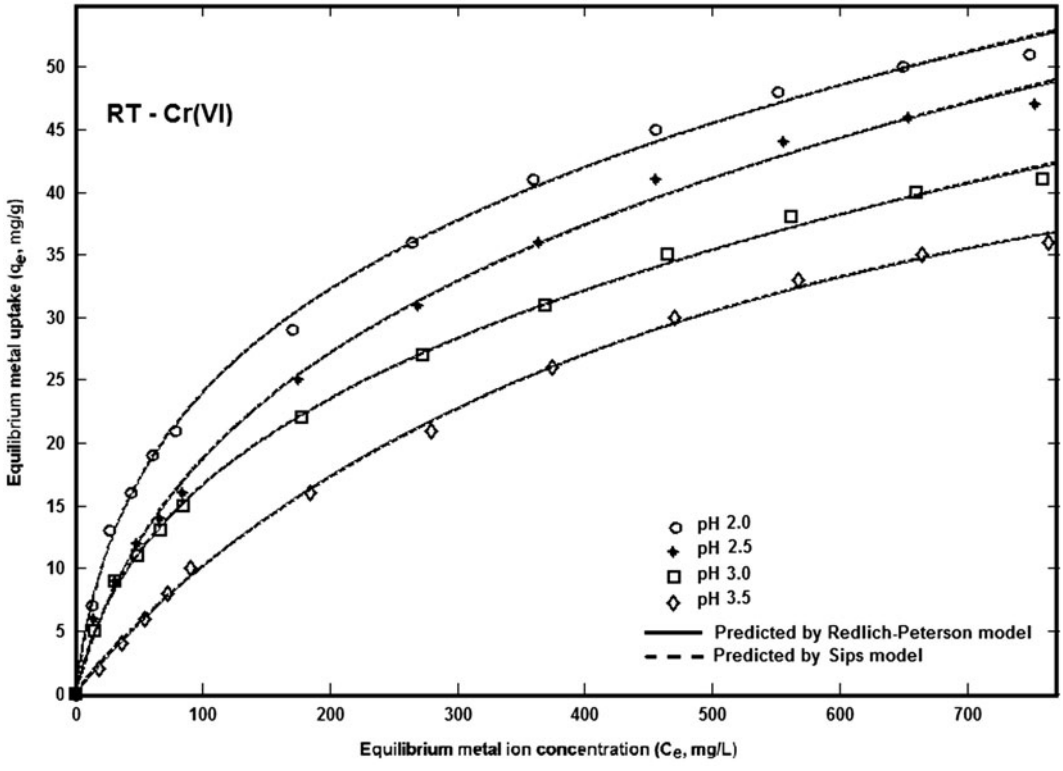

Fig. 6f. Adsorption isotherm model (3 parameter) fits for removal of Cr(VI) ions by RT.

Table 5d
Comparison of Langmuir monolayer capacity of the different adsorbents

Metal ions	Biosorbents	q_m (mg/g)	Refs.
Pb(II)	Tea industry waste	2.0	[34]
Pb(II)	Chitosan—polyacrylonitrile blend	20.08	[35]
Pb(II)	Cashew nut shell	17.82	[9]
Pb(II)	Hazelnut shell	28.18	[36]
Pb(II)	Saw dust	21.05	[37]
Pb(II)	Heartwood of Areca catechu powder	11.723	[38]
Pb(II)	Sugarcane bagasse treated by H_2SO_4	7.30	[39]
Pb(II)	Sugarcane bagasse	6.37	[39]
Pb(II)	*Rhizoclonium tortuosum*	**66.08**	**This study**
Ni(II)	Polyporous versicolor	57	[40]
Ni(II)	Chlorella miniata	1.4	[41]
Ni(II)	Chlorella vulgaris	0.6	[41]
Ni(II)	Tea industry waste	5.0	[34]
Ni(II)	Surface modified *Strychnos potatorum* seeds	74.55	[10]
Ni(II)	Mango peel	39.75	[42]
Ni(II)	Modified coir pith	38.9	[43]
Ni(II)	*Rhizoclonium tortuosum*	**85.09**	**This study**
Cr(VI)	Scenedesmus obliquus	15.6	[44]
Cr(VI)	Synechocystis sp.	19.2	[44]
Cr(VI)	Fly ash	23.86	[45]
Cr(VI)	Rice husk ash	25.64	[45]
Cr(VI)	Raw rutin	26.3	[46]
Cr(VI)	Rutin resin	41.6	[46]
Cr(VI)	*Rhizoclonium tortuosum*	**61.45**	**This study**

Note: The bold values indicate that the prepared material is for the present adsorption system.

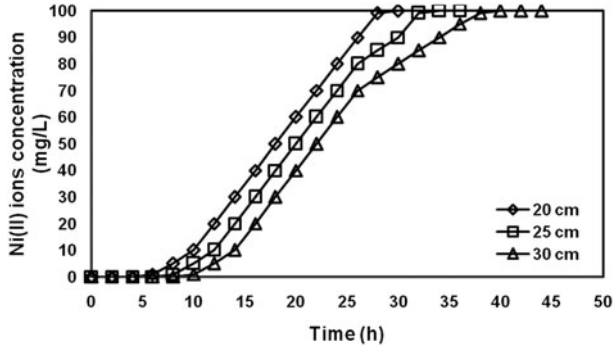

Fig. 7a. Effect of bed height on the removal of Ni(II) ions by RT.

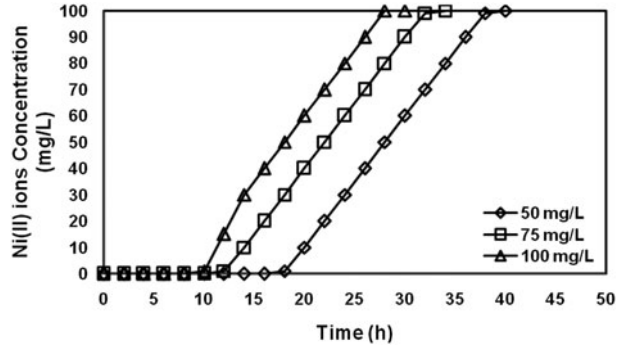

Fig. 7c. Effect of initial Ni(II) ion concentration on the removal of Ni(II) ions by RT.

depth service time (BDST) model. The column service time was selected as time when the effluent Ni(II) ions concentration reached 1 mg/L. Fig. 8a shows the BDST model plot for the removal of Ni(II) ions by algae biomass *R. tortuosum* (RT). The plot was drawn between the service time (h) and the bed height (cm) at a flow rate of 10 mL/min. The adsorption capacity of the bed per unit bed volume N_o was calculated from the slope of BDST plot. The rate constant K_a calculated from the intercept of BDST plot. The rate of solute transfer from the liquid phase to the solid phase was characterized by the rate constant K_a. The computed N_o was 4,016 mg/L for Ni(II) ions. The rate constant K_a was recorded as 0.0229 L/mg h. If K_a is large even a short bed will avoid breakthrough but as decreases a progressively longer bed is required to avoid breakthrough. The BDST model parameters can be useful to scale up the process for other flow rates without further experimental run.

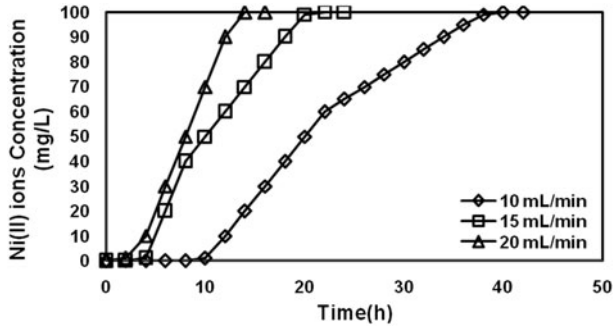

Fig. 7b. Effect of flow rate on the removal of Ni(II) ions by RT.

3.8.5. Thomas model

Thomas model plays an important role in the continuous flow conditions of column study to illustrate the dynamic behavior of column performance. The Thomas model is suitable for studying adsorption processes where limitations on external and internal diffusion were absent. Fig. 8b shows that the plot of ln $[(C_o/C_t) - 1]$ vs. t for the adsorption of Ni(II) ions onto adsorbent material *R. tortuosum* (RT) at different bed depths. By fitting the experimental values in this model, K_{th} and q_o values were calculated and the estimated values were shown in Table 7. From Table 7, it was observed that the adsorption capacity (q_o) of the Ni(II) ions is much higher for the column process compare to batch process, because higher concentration deferential between the metal ions in the liquid phase and the absorbent in the solid phase [49]. Table 7 shows that the value of K_{th} decreased with the increase of the bed depth, indicating that the mass transport resistance had increased and the correlation coefficients (R^2) are all greater than 0.90, theoretical and experimental q_o values are in accordance with each other. From the experimental data stated that the adsorption process have been well described by using the Thomas model.

3.9. Application to real effluents

The untreated nickel bearing electroplating effluent was collected from plating industry in Chennai, India. This effluent was characterized by considerable amount of light metals along with trace amount of heavy metals such as lead and copper. In the present study, the compatibility of adsorbent material *R. tortuosum* (RT) was tested with real industrial effluents. Initial solution pH plays an important role in the adsorption process. The adsorption of metal ions is increased with an increase in pH up to 4.5 and then decreased with further increase in pH. This may be due to the nature of binding groups present in the algae and solution chemistry of the metal ions used for the adsorption process [50]. The optimized algae material (RT) was employed for the treatment of plating effluent in the column mode experiment. This strategy was adopted to facilitate large scale application. Nickel bearing effluent with a Ni(II) ions concentration of 120 mg/L was adjusted to pH 4.5 and allowed to pass through the column containing the adsorbent material (RT). In order to regenerate the biosorbent an elution step was carried out (with 2 N NaOH) when the column reached saturation. In the

Table 6
Column data and their parameters obtained at different bed heights, flow rates and initial Ni(II) ions concentrations onto RT

Bed height (cm)	Flow rate (mL/min)	C_o (mg/L)	t_b (h)	t_e (h)	Δt (h)	V_{eff} (L)	q_{exp} (mg/g)	Ni(II) ions Removal (%)
Effect of bed height								
20	10	100	6	30	24	18	23.7	54
25	10	100	8	34	26	20.4	25.0	57
30	10	100	10	40	30	24	26.4	60
Effect of flow rate								
30	10	100	10	40	30	18	26.4	60
30	15	100	4	22	18	19.8	24.6	56
30	20	100	2	14	12	16.8	22.8	52
Effect of initial Ni(II) ion concentration								
30	10	100	10	40	30	18	26.4	60
30	10	75	12	34	22	21	25.5	58
30	10	50	18	28	10	28	24.2	55

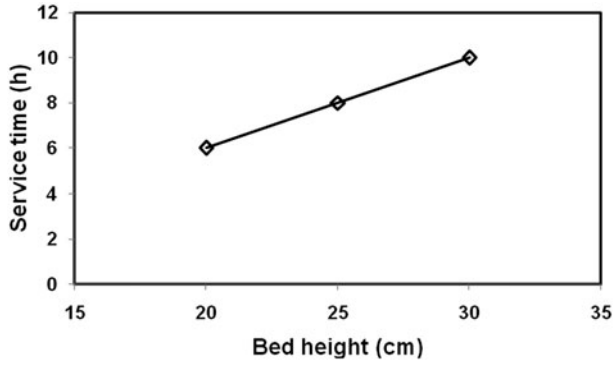

Fig. 8a. BDST model plot for the removal of Ni(II) ions by RT.

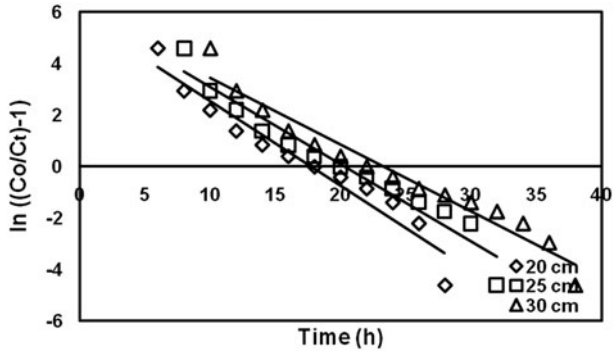

Fig. 8b. Thomas model plot for the removal of Ni(II) ions by RT.

Table 7
Thomas model parameters for Ni(II) ions adsorption onto RT at different bed depths

Bed depth (cm)	20	25	30
R^2	0.942	0.946	0.952
K_{th} (L/mg h)	0.00328	0.00299	0.00258
q_o (mg/g)	2.842	2.453	2.427

packed bed column, three adsorption–desorption cycles were completed in a continuous way. Fig. 9 shows the breakthrough curves for the removal of Ni (II) ions from industrial effluent using the adsorbent material (RT) in different cycles. The breakthrough time, exhaustion time, and Ni(II) ions uptake capacity for the three cycles are summarized in Table 8. From Table 8 results, it was observed that the breakthrough time and exhaustion time is decreased as the regeneration cycles progressed. The percentage removal of Ni(II) ions using adsorbent material (RT) were found to decrease in the successive cycles due to gradual

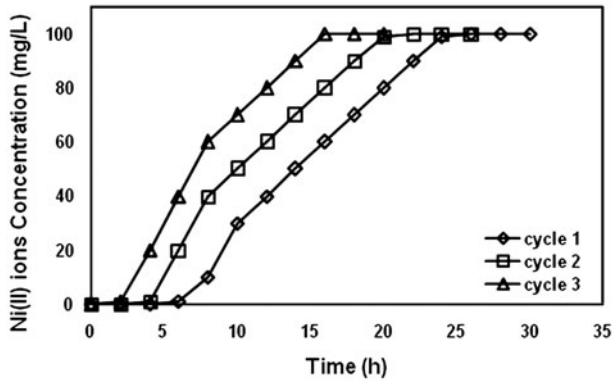

Fig. 9. Breakthrough curves for the removal of Ni(II) ions from industrial effluent using RT.

deterioration of adsorbent because of continuous usage. In the three cycles of adsorption about 4 L of plating effluent could be treated to reach the nickel standard (3 mg/L) established by the Central Pollution Control Board.

The breakthrough curves were attained quickly in the adsorption of Ni(II) ions using the adsorbent material (RT) due to the effect of high BOD and COD concentration in the plating effluents. The metal uptake capacity of the adsorbent material (RT) was reduced from 26 to 16 mg/L because of the presence of the organic matter in the plating effluents. After the completion of the process, the concentration of Ni(II) ions in the treated effluent was analyzed using an AAS (SL 176 Model, Elico Limited, Chennai, India), which was found to be 30 mg/L. To bring the Ni(II) ions concentration to a permissible limit (3.0 mg/L), the pH of the treated effluent was adjusted to 5.0 and then fed in the column setup. After one cycle of adsorption in the column, Ni(II) ions concentration of the effluent reached the permissible limit. Metal sorption largely depends on solution chemistry of the metals and competing ions in the liquid phase. The presence of considerable amount of lead and copper in effluent may have had a negative effect on nickel uptake as they compete in occupying the binding sites. For the duration of sorption experiments up to column exhaustion (in terms of nickel concentration) the exit concentrations of lead and copper were always below 100 μg/L. The excess amount of light metal ions (Na^+ and K^+) and total hardness (in terms of $CaCO_3$) in effluent may have influenced the binding of Ni(II) ion. Other parameters such as conductivity and total dissolved solids can also be cited as reasons for the significant deviation in nickel uptake from effluent. From Table 8, it was observed that the breakthrough time was decreased and the exhaustion time was increased as

Table 8
Column data and parameters obtained for plating industry effluents at optimum conditions using RT

Cycles	t_b (h)	t_e (h)	Δt (h)	V_{eff} (L)	q_{exp} (mg/g)	Ni(II) ions removal (%)	Desorption efficiency (%)
Cycle 1	6	26	20	15.6	21	47	60.80
Cycle 2	4	22	18	13.2	20	45	60.15
Cycle 3	2	16	14	9.6	18.6	42	59.55

cycles progressed. From the three cycles, it was examined that the adsorbent material (RT) is a relatively good adsorbent for the adsorption of Ni(II) ions from the effluent and no major decrease in bed height was observed at the three cycles.

4. Conclusion

In the present research work the adsorption ability of the algae biomass, *R. tortuosum* (RT) were tested for the removal of different toxic metal ions such as Pb (II), Ni(II), and Cr(VI) ions from aqueous solution. The batch adsorption process was affected by the different operating parameters such as biosorbent dose, pH, initial metal ions concentration, contact time, and temperature. These adsorption influencing parameters were optimized. The adsorption thermodynamics, kinetics, and equilibrium studies on the removal of metal ions by RT were explained at optimum conditions. The adsorption experimental data were fitted with nonlinear adsorption isotherm models such as Langmuir, Freundlich, Redlich–Peterson and Sips models. Sips model was identified as well-suitable isotherm model based on higher correlation coefficient and low error values. The maximum monolayer adsorption capacity of the *R. tortuosum* were found to be 66.08, 85.09, and 61.45 mg/g for Pb(II), Ni(II), and Cr(VI), respectively. The adsorption kinetic study was investigated using the pseudo-first-order, pseudo-second-order, and Elovich kinetic models. The adsorption kinetics followed the pseudo-second-order kinetic model. The thermodynamic parameter studies showed that the *R. tortuosum* have more competence on the adsorption of metal ions from aqueous solution and the results showed that the system is spontaneous, endothermic, and enthalpy driven. The column adsorption influencing parameters such as initial Ni (II) ions concentration, flow rate and bed height were optimized. The column experimental data were fitted with BDST and Thomas models. The RT material was successfully implemented for the removal of metal ions from synthetic wastewater. This results was further extended to the real industrial effluent treatment, i.e. the removal of Ni(II) ions from the nickel plating industrial wastewater was successfully carried out. The results from the present adsorption experimental studies reported that the *R. tortuosum* can be utilized as an effective low-cost biosorbent for the removal of metal ions from aqueous solution.

References

[1] P.S. Kumar, S. Ramalingam, R.V. Abhinaya, S.D. Kirupha, A. Murugesan, S. Sivanesan, Adsorption of metal ions onto the chemically modified agricultural waste, Clean—Soil, Air, Water 40 (2012) 188–197.
[2] P.S. Kumar, S. Ramalingam, V. Sathyaselvabala, S.D. Kirupha, A. Murugesan, S. Sivanesan, Removal of cadmium(II) from aqueous solution by agricultural waste cashew nut shell, Korean J. Chem. Eng. 29 (2012) 756–768.
[3] P.S. Kumar, C. Senthamarai, A. Durgadevi, Adsorption kinetics, mechanism, isotherm and thermodynamic analysis of copper ions onto the surface modified agricultural waste, Environ. Prog. Sustain. Energy 33 (2014) 28–37.
[4] P. Rajkumar, P. Senthil Kumar, S. Dinesh Kirupha, T. Vidhyadevi, J. Nandhagopal, S. Sivanesan, Adsorption of Pb(II) ions onto surface modified *Guazuma ulmifolia* seeds and batch adsorber design, Environ. Prog. Sustain. Energy 32 (2012) 307–316.
[5] C. Jeon, J.H. Cha, Removal of nickel ions from industrial wastewater using immobilized sericite beads, J. Ind. Eng. Chem. 24 (2015) 107–112.
[6] US Environmental Protection Agency (USEPA), Environmental Pollution Control Alternatives: Drinking Water Treatment for Small Communities, USEPA, Washington, Dc, 1990.
[7] C.A. Basha, K. Ramanathan, R. Rajkumar, M. Mahalakshmi, P.S. Kumar, Management of chromium plating rinsewater using electrochemical ion exchange, Ind. Eng. Chem. Res. 47 (2008) 2279–2286.
[8] P.S. Kumar, S. Ramalingam, R.V. Abhinaya, K.V. Thiruvengadaravi, P. Baskaralingam, S. Sivanesan, Lead(II) adsorption onto sulphuric acid treated cashew nut shell, Sep. Sci. Technol. 46 (2011) 2436–2449.
[9] P.S. Kumar, Adsorption of lead(II) ions from simulated wastewater using natural waste: A kinetic, thermodynamic and equilibrium study, Environ. Prog. Sustain. Energy 33 (2014) 55–64.
[10] K. Anbalagan, P.S. Kumar, K.S. Gayatri, S.S. Hameed, M. Sindhuja, C. Prabhakaran, R. Karthikeyan, Removal and recovery of Ni(II) ions from synthetic wastewater using surface modified *Strychnos potatorum* seeds: Experimental optimization and mechanism, Desalin. Water Treat. 53 (2015) 171–182.

[11] K. Anbalagan, P.S. Kumar, R. Karthikeyan, Adsorption of toxic Cr(VI) ions from aqueous solution by sulphuric acid modified *Strychnos potatorum* seeds in batch and column studies, Desalin. Water Treat. (in press), doi: 10.1080/19443994.2015.1049965.
[12] F. Fu, Q. Wang, Removal of heavy metal ions from wastewaters: A review, J. Environ. Manage. 92 (2011) 407–418.
[13] U.P. Kiruba, P.S. Kumar, C. Prabhakaran, V. Aditya, Characteristics of thermodynamic, isotherm, kinetic, mechanism and design equations for the analysis of adsorption in Cd(II) ions-surface modified Eucalyptus seeds system, J. Taiwan Inst. Chem. Eng. 45 (2014) 2957–2968.
[14] V.K. Gupta, A. Rastogi, Biosorption of lead from aqueous solutions by green algae Spirogyra species: Kinetics and equilibrium studies, J. Hazard. Mater. 152 (2008) 407–414.
[15] L. Deng, Y. Zhang, J. Qin, X. Wang, X. Zhu, Biosorption of Cr(VI) from aqueous solutions by nonliving green algae *Cladophora albida*, Miner. Eng. 22 (2009) 372–377.
[16] H. Javadian, M. Ahmadi, M. Ghiasvand, S. Kahrizi, R. Katal, Removal of Cr(VI) by modified brown algae *Sargassum bevanom* from aqueous solution and industrial wastewater, J. Taiwan Inst. Chem. Eng. 44 (2013) 977–989.
[17] B. Sarada, M.K. Prasad, K.K. Kumar, Ch.V.R. Murthy, Cadmium removal by macro algae *Caulerpa fastigiata*: Characterization, kinetic, isotherm and thermodynamic studies, J. Environ. Chem. Eng. 2 (2014) 1533–1542.
[18] F. Falaki, A. Fakhri, Adsorption properties of nickel oxide nanoparticles for removal of cango red from aqueous solutions, J. Phys. Theor. Chem. 10 (2014) 255–262.
[19] L. Khezami, R. Capart, Removal of chromium(VI) from aqueous solution by activated carbons: Kinetic and equilibrium studies, J. Hazard. Mater. 123 (2005) 223–231.
[20] A.S. Ozcan, S. Tunali, T. Akar, A. Özcan, Biosorption of lead(II) ions onto waste biomass of *Phaseolus vulgaris* L.: Estimation of the equilibrium, kinetic and thermodynamic parameters, Desalination 244 (2009) 188–198.
[21] Y.S. Ho, T.H. Chiang, Y.M. Hsueh, Removal of basic dye from aqueous solution using tree fern as a biosorbent, Process Biochem. 40 (2005) 119–124.
[22] N. Tewari, P. Vasudevan, B.K. Guha, Study on biosorption of Cr(VI) by *Mucor hiemalis*, Biochem. Eng. J. 23 (2005) 185–192.
[23] S. Lagergren, About the theory of so-called adsorption of soluble substances, Kungliga Svenska Vetensk Handl. 24 (1898) 1–39.
[24] Y.S. Ho, G. McKay, Pseudo-second order model for sorption processes, Process Biochem. 34 (1999) 451–465.
[25] M.J.D. Low, Kinetics of chemisorption of gases on solids, Chem. Rev. 60 (1960) 267–312.
[26] K. Vijayaraghavan, H.U.N. Winnie, R. Balasubramanian, Biosorption characteristics of crab shell particles for the removal of manganese(II) and zinc(II) from aqueous solutions, Desalination 266 (2011) 195–200.
[27] M.M.M. Rahmatia, P. Rabbani, A. Abdolali, A.R. Keshtkar, Kinetics and equilibrium studies on biosorption of cadmium, lead, and nickel ions from aqueous solutions by intact and chemically modified brown algae, J. Hazard. Mater. 185 (2011) 401–407.
[28] I. Langmuir, The adsorption of gases on plane surfaces of glass, mica and platinum, J. Am. Chem. Soc. 40 (1918) 1361–1403.
[29] H.M.F. Freundlich, Over the adsorption in solution, J. Phys. Chem. 57 (1906) 385–470.
[30] O. Redlich, D.L. Peterson, A useful adsorption isotherm, J. Phys. Chem. 63 (1959) 1024–1024.
[31] R. Sips, On the structure of a catalyst surface, J. Chem. Phys. 16 (1948) 490–495.
[32] D.H.K. Reddy, D. Ramana, K. Seshaiah, A.V.R. Reddy, Biosorption of Ni(II) from aqueous phase by *Moringa oleifera* bark, a low cost biosorbent, Desalination 268 (2011) 150–157.
[33] M. Sankar, G. Sekaran, S. Sadulla, T. Ramasami, Removal of diazo and triphenylmethane dyes from aqueous solutions through an adsorption process, J. Chem. Technol. Biotechnol. 74 (1999) 337–344.
[34] S.S. Ahluwalia, D. Goyal, Removal of heavy metals by waste tea leaves from aqueous solution, Eng. Life Sci. 5 (2005) 158–162.
[35] T. Anitha, P.S. Kumar, K.S. Kumar, B. Ramkumar, S. Ramalingam, Adsorptive removal of Pb(II) ions from polluted water by newly synthesized chitosan—Polyacrylonitrile blend: Equilibrium, kinetic, mechanism and thermodynamic approach, Proc. Saf. Environ. Prot. 98 (2015) 187–197.
[36] E. Pehlivan, T. Altun, S. Cetin, M.I. Bhanger, Lead sorption by waste biomass of hazelnut and almond shell, J. Hazard. Mater. 167 (2009) 1203–1208.
[37] Q. Li, J. Zhai, W. Zhang, M. Wang, J. Zhou, Kinetic studies of adsorption of Pb(II), Cr(III) and Cu(II) from aqueous solution by sawdust and modified peanut husk, J. Hazard. Mater. 141 (2007) 163–167.
[38] P. Chakravarty, N.S. Sarma, H.P. Sarma, Removal of lead(II) from aqueous solution using heartwood of *Areca catechu* powder, Desalination 256 (2010) 16–21.
[39] M.A. Martín-Lara, I.L.R. Rico, I. de la C.A. Vicente, G.B. Garcia, M.C. de Hoces, Modification of the sorptive characteristics of sugarcane bagasse for removing lead from aqueous solutions, Desalination 256 (2010) 58–63.
[40] F.B. Dilek, A. Erbay, U. Yetis, Ni(II) biosorption by *Polyporous versicolor*, Process Biochem. 37 (2002) 723–726.
[41] J.P.K. Wong, Y.S. Wong, N.F.Y. Tam, Nickel biosorption by two chlorella species, *C. Vulgaris* (a commercial species) and *C. Miniata* (a local isolate), Bioresour. Technol. 73 (2000) 133–137.
[42] M. Iqbal, A. Saeed, I. Kalim, Characterization of adsorptive capacity and investigation of mechanism of Cu^{2+}, Ni^{2+} and Zn^{2+} adsorption on mango peel waste from constituted metal solution and genuine electroplating effluent, Sep. Sci. Technol. 44 (2009) 3770–3791.
[43] A. Ewecharoen, P. Thiravetyan, W. Nakbanpote, Comparison of nickel adsorption from electroplating rinse water by coir pith and modified coir pith, Chem. Eng. J. 137 (2008) 181–188.

[44] G. Çetinkaya Dönmez, Z. Aksu, A. Öztürk, T. Kutsal, A comparative study on heavy metal biosorption characteristics of some algae, Process Biochem. 34 (1999) 885–892.
[45] A.K. Bhattacharya, T.K. Naiya, S.N. Mandal, S.K. Das, Adsorption, kinetics and equilibrium studies on removal of Cr(VI) from aqueous solutions using different low-cost adsorbents, Chem. Eng. J. 137 (2008) 529–541.
[46] N.A. Fathy, S.T. El-Wakeel, R.R.A. El-Latif, Biosorption and desorption studies on chromium(VI) by novel biosorbents of raw rutin and rutin resin, J. Environ. Chem. Eng. 3 (2015) 1137–1145.
[47] K.K. Wong, C.K. Lee, K.S. Low, M.J. Haron, Removal of Cu and Pb from electroplating wastewater using tartaric acid modified rice husk, Process Biochem. 39 (2003) 437–445.
[48] Z. Aksu, F. Gonen, Biosorption of phenol by immobilized activated sludge in a continuous packed bed: Prediction of breakthrough curves, Proc. Biochem. 39 (2003) 599–613.
[49] N. Atar, A. Olgun, S.B. Wang, S.M. Liu, Adsorption of anionic dyes on boron industry waste in single and binary solutions using batch and fixed-bed systems, J. Chem. Eng. Data 56 (2011) 508–516.
[50] P. Waranusantigul, P. Pokethitiyook, M. Kruatrachue, E.S. Upatham, Kinetics of basic dye (methylene blue) biosorption by giant duckweed (*Spirodela polyrrhiza*), Environ. Pollut. 125 (2003) 385–392.